DOI: 10.4408/IJEGE.2019-02.O-02

SLOPE ANALYSIS AND ROCK FALL ASSESSMENT IN THE KHINIS ARCHAEOLOGICAL AREA (KURDISTAN, NORTHERN IRAQ)

Emiliano DI LUZIO[(*)], Francesca COLOSI[(**)], Elisa FIDENZI[(**),(***)], Eva Savina MALINVERNI[(****)], Iolanda GAUDIOSI[(*)], Carlo Alberto BOZZI[(****),(*****)] & Roberto ORAZI[(**)]

[(*)] CNR - IGAG, Istituto di Geologia Ambientale e Geoingegneria, Area della Ricerca CNR RM1 Montelibretti - 00015 Monterotondo (Rome, Italy)
[(**)] CNR - ITABC, Istituto per le Tecnologie Applicate ai Beni Culturali, Area della Ricerca CNR RM1 Montelibretti - 00015 Monterotondo (Rome, Italy)
[(***)] Sapienza Università di Roma - Dipartimento di Storia, Disegno e Restauro dell'Architettura - Piazza Borghese, 9 - 00186 Rome (Italy)
[(****)] Università Politecnica delle Marche - Dipartimento di Ingegneria Civile, Edile e Architettura - Via Brecce Bianche, 12 - 60131 Ancona (Italy)
[(*****)] FieldTronics s.r.l. - Corso Garibaldi, 25 - 62012 Civitanova Marche (Macerata, Italy)
Corresponding author: emiliano.diluzio@igag.cnr.it

EXTENDED ABSTRACT

In questo lavoro vengono valutate, attraverso diverse metodologie di indagine geologica e geologico-tecnica, le condizioni di dissesto del versante roccioso che caratterizza l'area archeologica di Khinis, situata nell'Iraq nord-orientale, all'interno del territorio del Kurdistan. Processi di *rock fall* attivi a scala differente minacciano l'integrità e la conservazione del locale patrimonio culturale. Il sito conserva tracce significative dell'intensa attività scultorea rupestre prodotta durante il regno del re Assiro Sennacherib. Al passaggio tra l'ottavo e il settimo secolo a.C. vennero realizzati numerosi bassorilievi per celebrare la realizzazione delle imponenti opere di canalizzazione costruite per trasportare le acque correnti dalla catena dei Monti Zagros fino alla città di Ninive, la nuova capitale del regno Assiro. Il sistema di canalizzazione prendeva origine dall'area di Khinis, dove una serie di risorgive alimentava il Fiume Gomel che scorre ai piedi di un versante. Le sculture parietali a bassorilievo, ricavate entro una potente successione calcarenitica paleogenica, rappresentano un caso eccezionale di conservazione dell'arte monumentale assira. In ragione di questo, per il sito archeologico e l'intero sistema di canalizzazione assiro verrà proposta la candidatura nella lista del patrimonio culturale UNESCO (*World Heritage List*).

Grazie alla collaborazione tra geologi, architetti, archeologi ed esperti in sistemi di acquisizione di dati telerilevati è stato completato uno studio multi-disciplinare, iniziando da un rilievo aero-fotogrammetrico del versante roccioso tramite un sistema a pilotaggio remoto. In seguito, l'analisi strutturale e geomeccanica dell'ammasso roccioso e delle superfici di debolezza strutturale ha permesso di realizzare una modellazione geometrica di due pilastri di roccia di grandi dimensioni (700-900 m^3) presenti al margine del pendio. Uno di questi blocchi contiene il Grande Bassorilievo, un'opera scultorea che rappresenta una scena di saluto rituale tra il sovrano Sennacherib e la suprema coppia divina del pantheon Assiro, il dio Aššur e la dea Mullissu/Ninlil. L'altro blocco si ritrova invece ai margini di un'area di cava dismessa, utilizzata come fonte di approvvigionamento di materie prime per la realizzazione delle canalizzazioni, oggi sepolte e tombate sotto una coltre di materiale detritico e alluvionale. Considerando la deformazione fragile dell'ammasso roccioso, caratterizzata da pochi elementi di discontinuità di grande estensione e spaziatura, le condizioni di stabilità dei due pilastri sono state analizzate adottando un metodo all'equilibrio limite. I potenziali fattori di innesco dei processi di instabilità e crollo, quali sollecitazioni sismiche e infiltrazioni di acqua meteorica, sono stati valutati attraverso analisi di sensibilità, nel quadro delle condizioni sismotettoniche e climatiche dell'area.

Il sito archeologico é interessato anche da eventi di *rock falls* che implicano il distacco di blocchi calcarenitici di due ordini di grandezza più piccoli (2-4.5 m^3) da pareti verticali situate nella parte sommitale e mediana del versante. Tali processi sono stati simulati attraverso una modellazione di tipo cinematico e probabilistico. Un inventario dei blocchi osservati a riposo sia sui settori a media pendenza del versante che ai piedi dei bassorilievi, è stato utilizzato come vincolo principale per il calcolo iterativo e la validazione del modello (modalità di *back-analysis*). I risultati della modellazione statistica hanno permesso di prevedere le traiettorie dei blocchi - distinguendo le fasi di roto-traslazione da quelle di rimbalzo e volo - e le aree principali di accumulo, e di definire inoltre le distanze di run-out e i parametri cinematici del moto di propagazione. L'integrazione di un *design block*, vale a dire di un blocco di progetto di dimensioni stimate in seguito a misurazioni sulle pareti rocciose, ha permesso di valutare i valori energetici coinvolti nei processi di rock fall, valori necessari alla progettazione di un piano di mitigazione del dissesto in conformità con i requisiti di conservazione del valore paesaggistico del sito.

Infine, il lavoro presenta alcune ipotesi originali riguardo le possibili relazioni tra i processi di instabilità parietale e un'opera scultorea assira rinvenuta alla base del pendio di Khinis, dove si possono osservare alcuni blocchi di roccia scolpiti, frammentati e ruotati lungo le sponde del Fiume Gomel. Originariamente questi blocchi appartenevano ad un grande monolite recante bassorilievi raffiguranti il re Sennacherib e le divinità Assire. I processi di *rock fall* attivi nell'area vengono discussi sia come potenziale risorsa di materiale litoide per la realizzazione dell'opera che come causa prevalente delle attuali condizioni di dissesto. Le interrelazioni tra processi naturali e opere antropiche costituiscono un motivo di ulteriore interesse per la preservazione e la valorizzazione dell'area archeologica di Khinis.

ABSTRACT

This work assesses the conditions of slope instability in the Khinis archaeological area (northern Iraq), which threaten the integrity and conservation of the local cultural heritage. The site preserves traces of sculpturing activity produced during the reign of the Assyrian king Sennacherib (VIII-VII centuries BCE, i.e. before common era). Bas-reliefs were created to celebrate the realization of canalization works built to transport waters from the Zagros Mountains to Nineveh.

Multidisciplinary analysis of the local rock slope highlights active rock fall processes of varying magnitude. A few large rock pillars (hundreds of m^3) show different conditions of instability after a limit-equilibrium analysis. Meanwhile, potential falls of smaller rock blocks affect the entire Khinis slope as they can detach from mid-slope escarpments. Through probabilistic 3D modelling, the calculation of block trajectories, arrest areas and energy values involved allows the design of a remediation plan, in accordance with the preservation requirements of the landscape value of the site.

Finally, some hypotheses are advanced concerning the possible relationships between rock fall processes and the accomplishment of some of the Assyrian sculptures. A reason for further interest in this archaeological site, that it will soon be proposed for inclusion in the UNESCO World Heritage List.

Keywords: *slope analysis, rock fall, Khinis, Assyrian heritage, Kurdistan, Iraq*

INTRODUCTION

The Khinis archaeological area is located in the Kurdistan region (northern Iraq), approximately 70 km north-east of the city of Mosul and along the southern piedmont area of the Zagros fold-and-thrust belt. The site is the largest and most elaborate rock complex of ancient Assyria and represents a celebratory and decorative apparatus that accompanied the construction of an articulated canal system branching from the River Gomel (Bachmann, 1927; Bär, 2006; Reade & Anderson, 2013). This system was built for the Assyrian king Sennacherib in the VIII-VII centuries BCE to bring water to his new capital Nineveh, which is modern Mosul (Fig. 1a).

The hilly landscape at Khinis is characterized by a Paleogene, thick turbiditic sequence composed of well-bedded calcarenites and breccias shaped by fluvial and aeolian erosion (Fig. 1b). Sub-vertical rock escarpments host outstanding elements of the local cultural heritage, including bas-reliefs and niches that are the maximum expression of Assyrian rock art, both in size and quality of execution (Figs. 2a-e). Considering these geoarchaeological characteristics, the Khinis site can be associated with the concept of 'geoheritage' which describes areas where the geological and geomorphological features have scientific, cultural, historical and educational value (Panizza, 2001; Panizza & Piacente, 2005; Reynard, 2005; Reynard & Giusti, 2018).

The preservation and development of the archaeological area are threatened by rock slope instabilities including diffuse rock fall processes from the slope overhanging the River Gomel and possible detachment of isolated, very large rock masses. Similar rock failure events are recognized in the nearby mountain regions (Othman & Gloaguen, 2013; Yousif & Shakir, 2015).

Therefore, the main goal of this study was the assessment of geological hazards posed by rock fall activity and the development of a remediation plan. Based on cooperation between geologists, architects, archaeologists and experts in remote sensing data acquisition and elaboration systems, a multi-disciplinary study was completed, including i) UAV (unmanned aerial vehicle) surveys for the aero-photogrammetric reconstruction of the slope topography; ii) structural and geomechanical analyses of the jointed rock masses; iii) geometric modelling and stability analyses of isolated rock blocks with insights into possible triggering factors; iv) 3D probabilistic rock fall modelling; and v) sizing of mitigation operas consisting in rock fall barriers.

Geometric models of two rock blocks of great dimensions (700-900 m^3) were outlined on the slope edge (named A and B in Figs. 1b, 2a). One of these blocks hosts the Great Relief, a bas-relief representing a ritual greeting scene featuring the sovereign Sennacherib and the supreme divine couple of the Assyrian pantheon, the god Aššur and goddess Mullissu/Ninlil. (Figs. 2b, c). Considering the very low-grade brittle deformation into the rock mass, stability conditions were evaluated adopting a limit-equilibrium method. Potential triggering factors, such as seismic vibrations and rainwater infiltration, were investigated through sensitivity analyses and discussed considering the seismotectonic setting and climate conditions of north-eastern Iraq.

Evidence of past failure events was analysed and connected to Assyrian sculptures at the base of the Khinis slope, where a broken and tilted rock block bearing bas-reliefs depicting King Sennacherib is found along the River Gomel (Fig. 2e). Relationships between rock fall events, realization and present state of this sculptured monolith were also investigated.

Diffuse rock falls involving blocks two orders of magnitude smaller (2-4.5 m^3) were simulated through 3D modelling (e.g., Scioldo, 1991, 2006; Agliardi & Crosta, 2003; Dorren, 2003; Crosta & Agliardi, 2004; Guzzetti *et alii*, 2002; Lan *et alii*, 2007) based on a probabilistic approach (see Li & Lan, 2015 for a review). An original inventory of calcareous blocks, found resting on both the mid-slope sectors and feet of bas-reliefs, was used as a main constraint for iterative calculation and modelling validation (back-analysis mode). Modelling results allowed the prediction of block trajectories, accumulation areas, run-out distances and kinematic parameters of falling blocks.

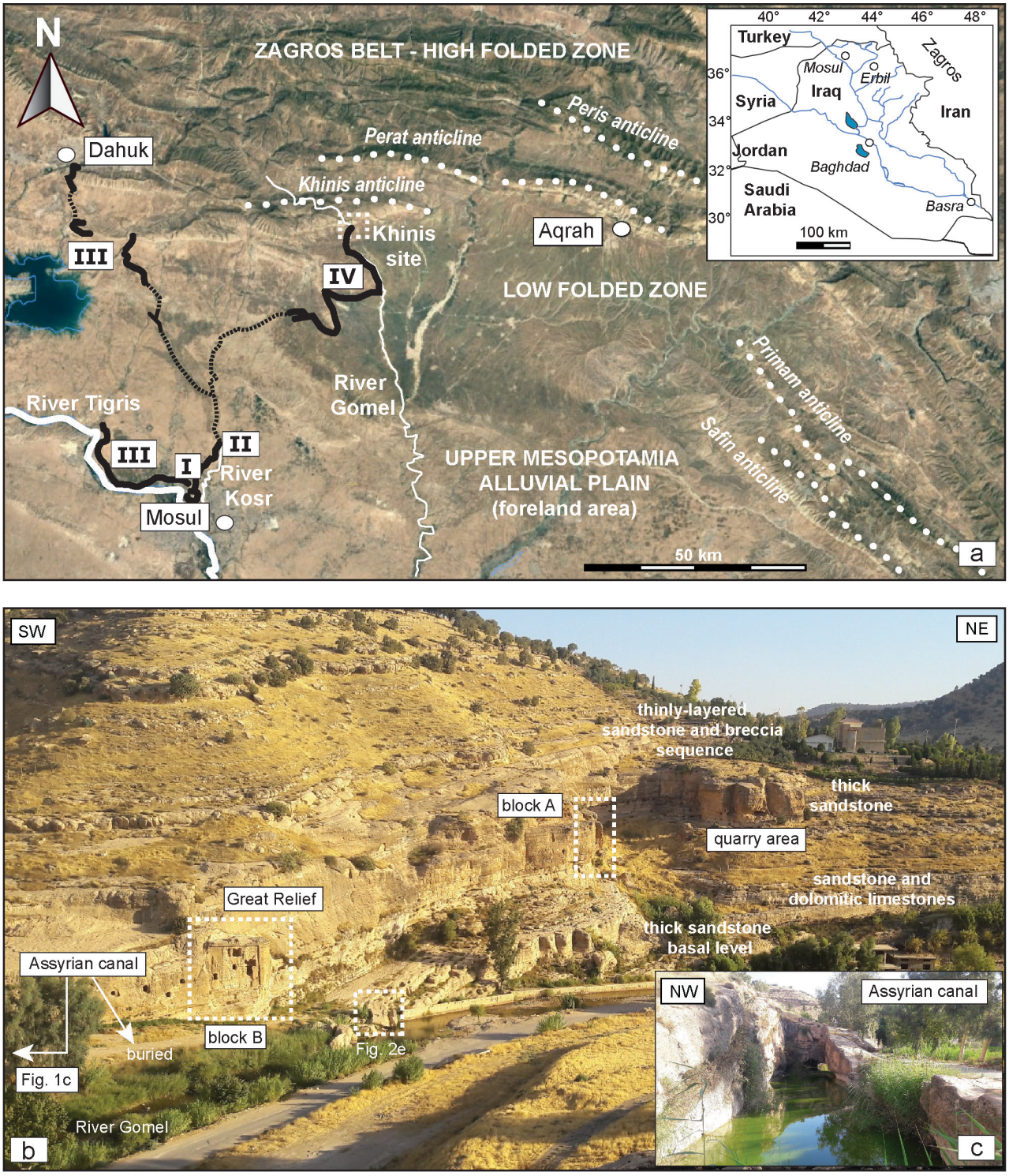


Fig. 1 - a) Location of the Khinis site in northern Iraq, Kurdistan region. The Sennacherib canal system, which was realized in four phases (I-IV) over the VIII-VII centuries BCE, is traced by thick black lines (from Morandi Bonacossi, 2018); canalized wadis are reported as thin, black dashed lines; the Gomel and Tigris rivers are highlighted in white; the axes of main anticlines within the Low-Folded Zone of the Zagros belt are evidenced by white dotted lines; b) panoramic view of the Khinis archaeological area, the local sedimentary sequence, the River Gomel and the buried Assyrian canal. Rock blocks A and B - this last with the Assyrian Great Relief - are evidenced; c) uncovered stretch of the canal west of the study area

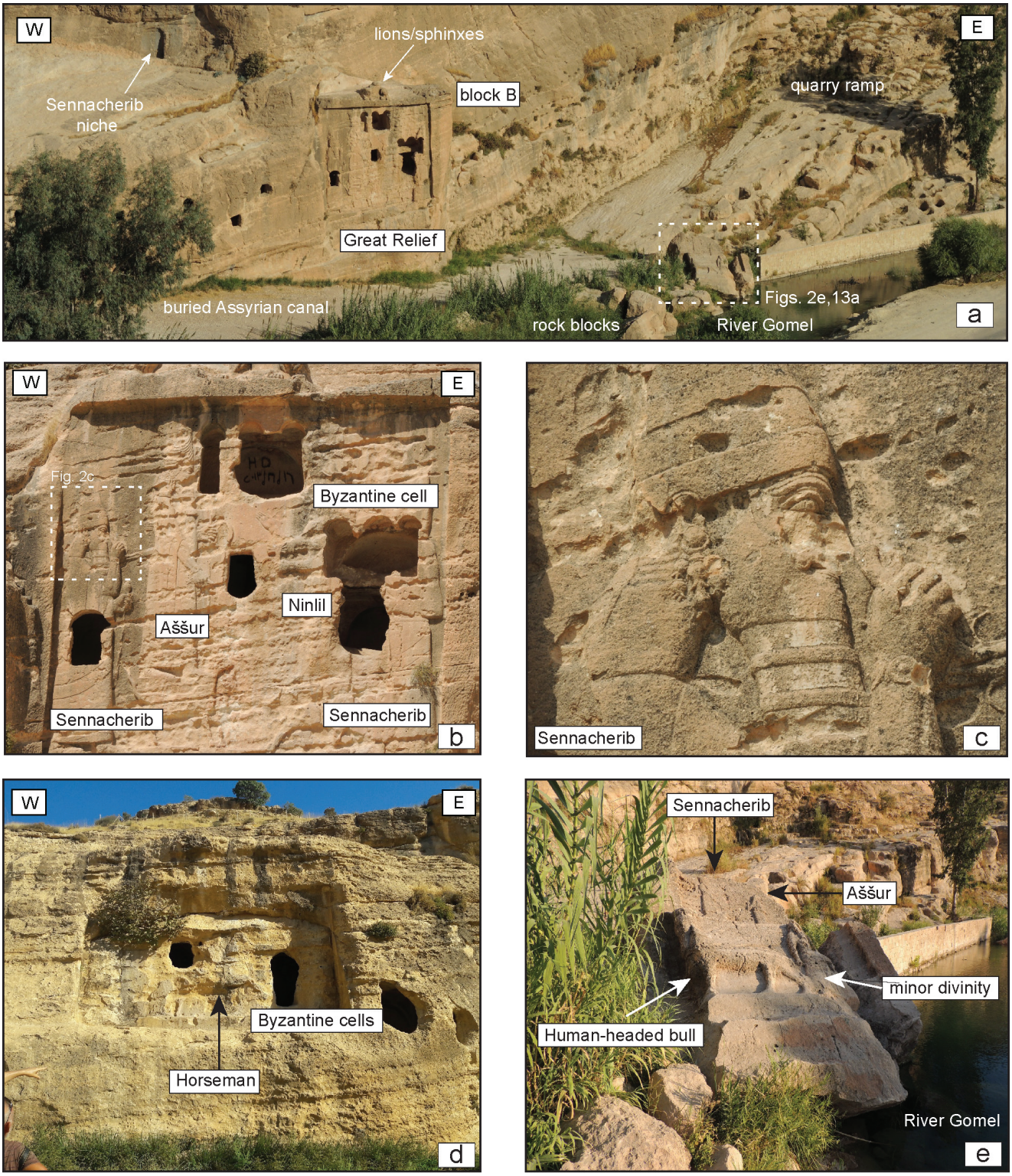


Fig. 2 - a) Particular of the Khinis rock slope with the Great Relief, one of the 13 niches depicting Sennacherib and the quarry ramp; b) the Great Relief imaging on both edges king Sennacherib facing god Aššur and goddess Mullissu/Ninlil; c) particular of Sennacherib's face; d) the Horseman Relief (see location in Figs. 5c, 6b); e) broken and tilted rock block found in the River Gomel with other Assyrian bas-reliefs

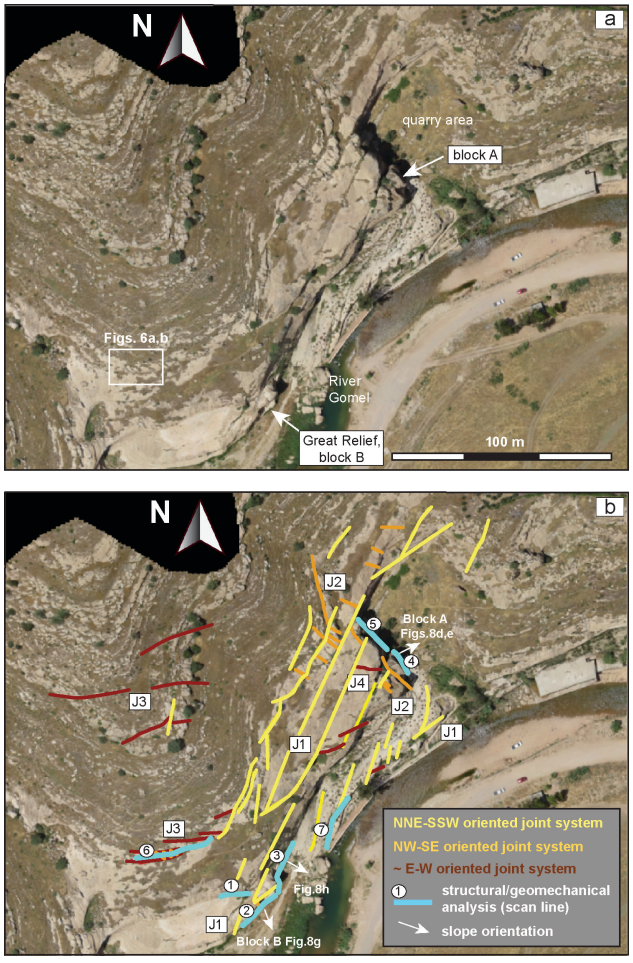


Fig. 3 - a) Orthoimage of the Khinis area from the UAV survey; b) line drawing of the main joint systems (J1-J4) identified at the slope scale. Locations of 1-7 scan lines and slope orientations are reported

Afterwards, a countermeasure plan was also defined considering the need for aesthetic preservation of the local landscape. Actions for site conservation are part of the range of initiatives to advance the proposal for the inclusion of Sennacherib's irrigation network and therefore the Khinis archaeological area in the UNESCO World Heritage List (WHL) (Orazi, 2019).

GEOLOGICAL SETTING

The Khinis area is close to the boundary between the High Folded and Low Folded zones of the Zagros belt (Jassim & Goff, 2006; Zebari, 2013). This structural distinction corresponds to a geomorphological transition from high-elevation mountainous areas (1000-3000 metres a.s.l.) to a piedmont junction zone with low-elevation topography (500-900 metres a.s.l.). Here, hilly ridges oriented NW-SE and WNW-ESE are the morpho-structural signature of elongated, low-amplitude anticlines composed of Tertiary marine sedimentary rocks (Buday & Jassim, 1987; Alawi, 2004; 2007; Ghasemi & Talbot, 2005; Jassim & Goff, 2006; Blanc *et alii*, 2003; Aqrawi *et alii*, 2010; Csontos *et alii*, 2012; Sissakian & Fouad, 2012; Koshnaw *et alii*, 2017: Le Garzic *et alii*, 2019). These anticlines are separated by broad synclines forming wide and expanded plains (Fig. 1a). The morpho-structural framework is complicated by normal and strike-slip regional faults, parallel or sometimes transverse to the main compressional structures, which have influenced the river drainage networks and alluvial valley orientations (Stevanovic, 2009; Stevanovic *et alii*, 2009).

The sedimentary sequence at Khinis crops out on the southern flank of a main anticline (Fig. 1a) featuring a southwest-dipping monocline with an average dip of 15-20° (Fig. 1b). A basal level of thick calcareous sandstones is overlain by a heterogeneous interval containing sandstones and dolomitic limestones, in turn passing upwards to a massive or thick-bedded sandstone (dark-grey calcarenite) layer featuring sub-vertical rock cliffs. This last unit underlies thin-bedded calciturbidites and breccias. The whole sedimentary sequence belongs to the middle-late Eocene "Spina Pi" Formation; sedimentary structures, petrographic analyses and lithofacies associations refer to marine sedimentation controlled by a gravity-flow regime and turbiditic currents (Polla, 2011; Al-Mashaikie & Latif, 2017).

The Khinis rock slope is disrupted by mechanical discontinuities associated with bedding (*S0*) and three prevailing sets of joints and mega-joints. Joints are numerous near the slope edge (Fig. 3a), where the prevailing system is oriented NNE-SSW and characterized by a limited number of regularly spaced (approximately 10 m apart), vertical or sub-vertical fractures with considerable length (up to 100 m). Another system of joints oriented NW-SE shows a main concentration on the south-western edge of a disused Assyrian quarry. The structural framework is completed by discontinuities that are concentrated in the western sectors with orientations ranging from WNW-ESE to ENE-WSW (Fig. 3b).

ARCHAEOLOGICAL BACKGROUND

The region of Iraqi Kurdistan is an arid territory in which, due to the low rainfall and high temperatures, the Assyrians watered crops by means of irrigation canals. The monumental complex of Sennacherib consists of canal systems built by Assyrian rulers in four different phases over the period from the VIII to the VII centuries BCE. The hydraulic network reached an overall length of 150 km. Canals and canalized wadis conveyed water from the larger streams and piedmont springs to the Kosr River, which traversed the city of Nineveh before flowing into the Tigris, and supplied water to the surrounding lands through a well-organized distribution system (Fig. 1a). At the heads of the

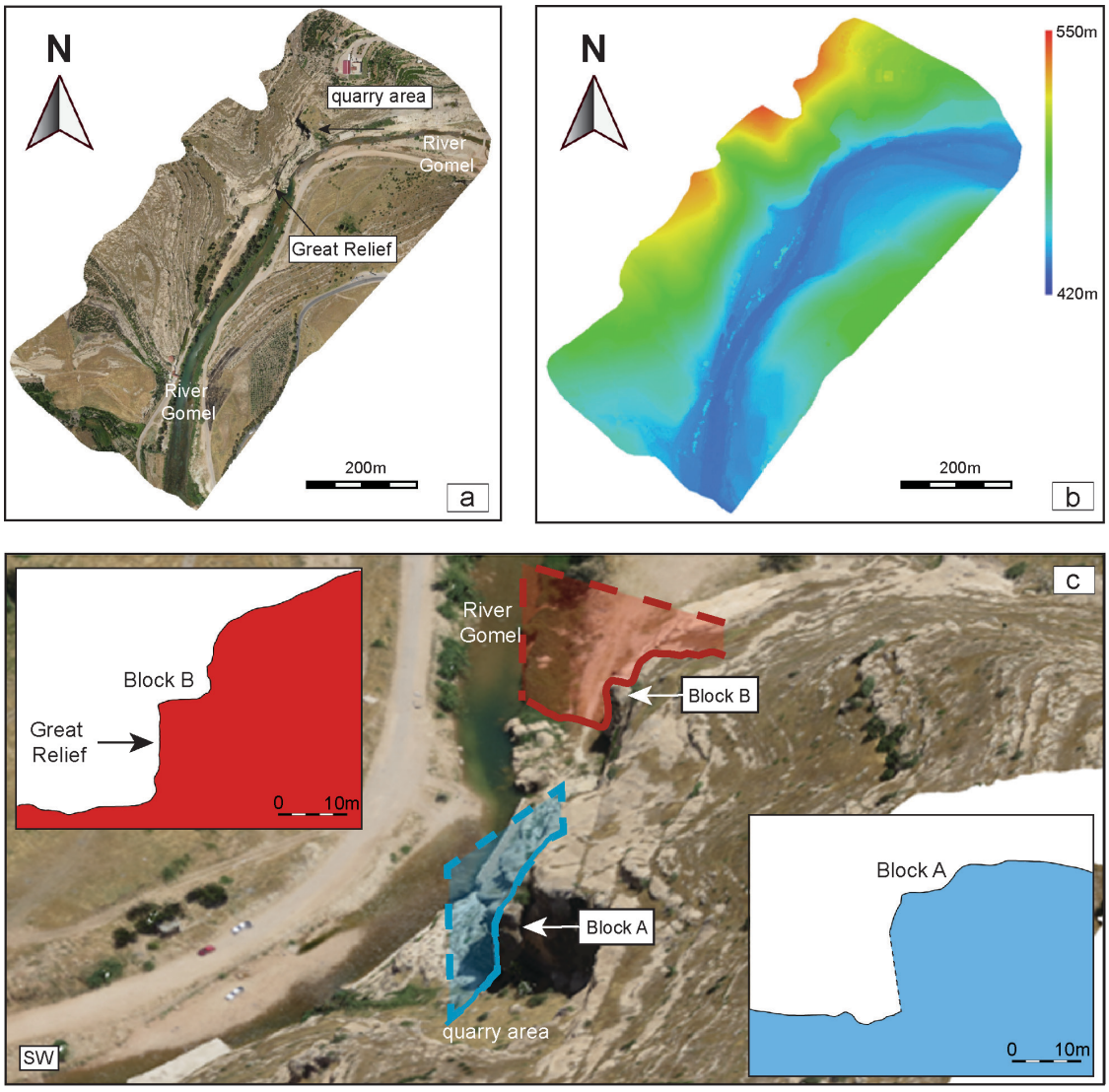


Fig. 4 - a) Enlarged orthoimage of the Khinis area from the UAV survey; b) digital elevation model; c) 3D image elaborated by JRC Reconstructor® software and topographic sections through blocks A and B

canals, along their paths and in the adjacent areas, the hydraulic structures were accompanied by commemorative inscriptions and ornamental rock-face bas-reliefs (Jacobsen & Lloyd, 1935; Oates, 1968; Reade, 1978; Bagg, 2000; Ur, 2005; Orazi, 2019).

The fourth construction phase is certainly the most impressive, and it is the phase that has survived best until today. The canal system had its starting point at the Khinis site (Figs. 1b, 2a), where the commemorative complex includes two carvings of monumental proportions, the Great Relief and the Horseman Relief, and thirteen niches featuring King Sennacherib in low relief (Figs. 1b, 2a-d). On the same slope edge, a series of cells (Fig. 2b) was carved into the rock by pioneering monks in the Byzantine Age (Bachmann, 1927).

The Great Relief dominates the point where a water canal once branched off from the River Gomel. Currently, the canal is almost completely buried under alluvial, debris and infill deposits, except for a still uncovered part visible a few tens of metres to the west of the study area (Fig. 1c). The rock panel (9.28 × 9.03 m) represents the sovereign Sennacherib - sculpted at both edges - and the supreme divine couple of the Assyrian pantheon, the god Aššur and his consort goddess Mullissu/ Ninlil, shown standing above their symbolic animals (Figs. 2b, c). Two lion/sphinx bases right above the panel (Fig. 2a) must once have supported statues or a columned building (Fales & Del Fabbro, 2015; Morandi Bonacossi, 2018).

The so-called Horseman Relief is characterized by a

rectangular panel that originally contained a large Akkadian inscription placed at the centre and framed laterally by two mirror-image figures of Sennacherib. The relief was subsequently reworked: in its centre, a figure of a knight was sculpted mounted on his steed, with a spear lowered (Fig. 2d). This intervention dates to the post-Assyrian period and has largely obliterated the original Assyrian relief (Reade & Anderson, 2013).

Along the northern (right) bank of the River Gomel a tilted block lies broken next to other smaller rock blocks (Figs. 2a, e). On the side overlooking the river, the relief is divided into two registers: the lower register shows a minor divinity flanked by two gate-protector genies represented by human-headed bulls (lamassu); the upper register portrays King Sennacherib in adoration before the god Aššur (Morandi Bonacossi, 2018).

Finally, the north-eastern bank of the River Gomel is characterized by the presence of a rock quarry (Bachmann, 1927; Jacobsen & Lloyd, 1935) (Fig. 1b). The ramp shown in Fig. 2a was built following the bedding of the geological substratum and used by quarrymen to slide blocks from the extraction area towards the river.

METHODOLOGIES

Remote sensing and UAV data acquisition

Remote sensing and UAV data were used for covering different scales of representation for a detailed documentation of the Khinis site and to obtain a 3D model of the rock slope. First, Pleiadés satellite, VHR panchromatic (0.5 m) and multispectral (2 m) images were used to produce maps at medium scales: a vector/raster map and a DEM (Malinverni *et alii*, 2017). Then, to document the entire archaeological area in more detail, a UAV survey was applied. Through a SenseFLY Swinglet drone system equipped with a Canon IXUS 127 HS camera (focal length 4.3 mm), 88 stereoscopic images were taken at a flight altitude of 171 metres asl, obtaining a ground resolution of 4.89 cm/px.

Selected frames were processed using Agisoft Photoscan, a 3D data processing software based on the Structure From Motion technique. The program reworked the frames into a single, high-density point cloud (containing 56.882.644 points processed in High quality and Aggressive Depth filtering). This was subsequently scaled and geo-referenced through thirteen ground control points surveyed by the GNSS RTK mode with a Topcon GR-5 receiver.

Successively, the point cloud was converted into a mesh (composed by 9.862.016 faces and 4.937.861 vertices) that was textured with a photographic definition. The mapped and georeferenced surface was exported into JRC 3D Reconstructor, a software that manages 3D data, to create a high-definition orthophoto of the Khinis area surrounding the River Gomel (Fig. 4a) and a DEM (Fig. 4b) with a resolution of 20 cm/px and a point density of 25 points/m². Several 2D vertical sections of blocks A and B (Fig. 4c) were extracted from JRC 3D Reconstructor, which were used to calculate dimensions and volumes.

Moreover, horizontal sections of the whole 3D surface were used to obtain 1m elevation contour lines and the planimetric mapping of the Khinis area (see also Fig. 12a). The plan of the area was essential to draw up the project for the use of the site which includes the definition of pedestrian paths and vehicular routes for visitors, toilets, parking lots and parking areas. Finally, elevation contour lines were imported in the Rotomap® software to simulate the slope topography and run the rock fall modelling.

Rock slope and brittle deformation analysis

The physical behaviour of a rock mass depends on the combined strength characteristics of the matrix and the discontinuities. The relative weights of these two factors are determined by the characteristics of brittle deformation and the intensity of fracturing, commensurate with the scale of examination. In the case of the Khinis rock slope, the fracture network includes a few discontinuities of great extent (even tens of metres in length) spaced one to several metres apart; rock masses between them appear substantially undeformed (Figs. 3a, b). Based on this evidence, a discontinuous approach to slope analysis was adopted in this study; rock masses were considered undeformed discontinuous media delimited by main discontinuities (joint systems and S0) along which movements could take place. The brittle deformation field affecting the Khinis rock slope was analysed along 7 scan lines (Fig. 3b); joint systems were distinguished and characterized according to the standards from Ulusay & Hudson (2007).

Equilibrium method analysis and discontinuity strenght evaluation

The choice of a discontinuous approach to slope analysis implied that the geometric and strength characteristics of discontinuities were regarded for assessing potential instabilities. Therefore, a limit equilibrium method was applied for the stability analysis of rock blocks A and B observed on the Khinis slope face using the RocScience® software suite. The mechanical behaviour of discontinuities was evaluated adopting the Barton & Choubey (1977) criterion, suggesting that the effective shear strength of discontinuities depends upon three components: i) the residual friction (φr); ii) the surface roughness, a geometric component expressed through the joint roughness coefficient (*JRC*); and iii) the resistance to breakage of asperities on the discontinuity surface, defined by the ratio $JCS/\sigma'n$, where σ'n is the effective normal stress applied and *JCS* is the joint compressive strength. *JCS* values (MN/m²) were obtained in this study from sclerometric measurements on main discontinuities taken with a Schmidt hammer at sites 1-7, where the *JRC* values were also estimated by comparing joint

	Block A	Block B
Discontinuities	*Basal joint (J2 set)*	*Bedding (S0)*
JCS	*42 MPa*	*55 MPa*
JRC	*14 (averaged 7 profiles)*	*6 (averaged 5 profiles)*
Φb	*30°*	*30°*
r	*26.9 (averaged 11 values)*	*32.8 (averaged 8 values)*
R	*31.6 (averaged 11 values)*	*34.3 (averaged 8 values)*
Φr	*27°*	*29°*

Tab. 1 - Strength parameters adopted for characterization of discontinuities controlling potential failures of block A and B

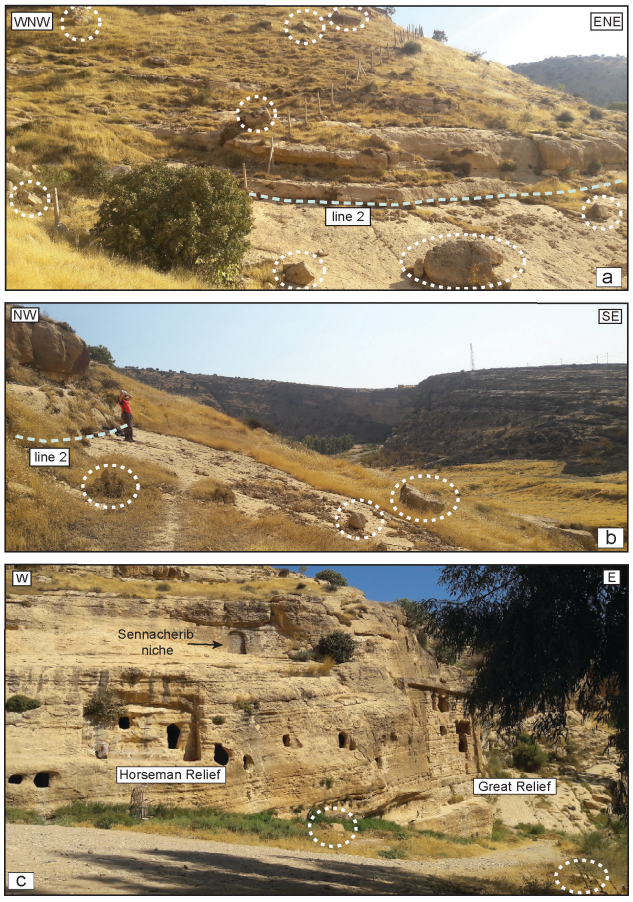


Fig. 5 - Dotted, white circles include detached rock blocks found resting on: a), b) the Khinis slope (starting line 2 in the rock fall modelling is indicated); c) the flat area between the slope base and the River Gomel

roughness profiles with standard profiles. The residual friction angle was determined following the Barton & Choubey (1977) equation (1): $\varphi r=(\varphi b-20°)+ 20(r/R)$, where: φb is the basic friction angle, i.e., the angle of friction for perfectly smooth and polished surfaces (for the Khinis calcarenites, φb = 30° was assumed considering literature values from Hoek & Bray, 1981; Cruden & Hu, 1988; Bruce *et alii*, 1989; Goodman 1989; Gonzales de Vallejo *et alii*, 2005; Waltham, 2009); *r* is the number of Schmidt hammer rebounds on an altered surface; and R the number of Schmidt hammer rebounds on the same polished surface, with *R*>*r*. Strength parameters assumed for potential failure surfaces of block A and B (later discussed) are reported in Table 1.

Rock block inventory and modelling assumptions

Several rock blocks were observed in the field resting on the Khinis slope (Figs. 5a, b), while others were found between the base of the escarpment and the River Gomel (Fig. 5c). With the aid of UAV-derived images and through GPS measurements, a geo-referenced block inventory including 83 elements was completed; in the course of their descent, 54 of the surveyed rock blocks stopped on the inclined slope, whereas 29 reached the valley floor and stopped there (Fig. 6a). Such evidence should not be considered fully representative of the phenomenon since some blocks may have been removed or fallen into the River Gomel.

Down-slope propagation of rock blocks was simulated with the Rotomap® software code (Scioldo, 2006), which implements a probabilistic model by calculating a large number of 3D trajectories and adopting a lumped mass approach; i.e., only the boulder centre of mass is tracked (kinematic modelling). Therefore, the effects on trajectories of block size and shape, which, as in this case, are often difficult to determine exactly, were neglected (e.g., Ritchie, 1963; Evans & Hungr, 1993; Guzzetti *et alii*, 2002; Agliardi & Crosta, 2003; Dorren, 2003; Lan *et alii*, 2007).

For the assessment of model inputs, the following assumptions were made: i) block starting points were set at the bases of three mid-slope escarpments having an average height (*H*) of 3 metres (lines 1-3 in Fig. 6b); ii) initial velocities $V0min$= 4.1 m/s and $V0max$=5.75 m/s were calculated by equation (2): $V0min,max=Cs\sqrt{(2gHmin,max)}$, considering detachment heights *Hmin* and *Hmax*=1.5 and 3 m and coefficient *Cs*=0.75 for non-vertical detachment scarps; and iii) a symmetrical angular deviation of 10° from the line of maximum slope during initial motion was imposed to account for the observed rock fall dispersion.

Three terrain classes were identified (slope zonation) by interpretation of UAV-derived images and field surveys (Fig. 6a). These classes were i) exposed calcareous rock (ECR); ii) shrub-like vegetation (SLV) and iii) the River Gomel (RG). Then, following a literature review, initial values of normal and tangential elastic restitution coefficients (*Kn* and *Kt*, respectively) and dynamic friction angle (Φd) were assigned to each terrain class to account for the loss of energy during bouncing and rolling phases of motion (Tab. 2). Theoretically, the River Gomel was assigned very low *Kn* and *Kt* values and a very high friction angle to forcefully arrest rock blocks falling into the water.

A total of 272 trajectories were then simulated. Modelling calibration through a back-analysis procedure was performed by slightly varying *Kn*, *Kt* and Φd values and constraining intermediate results to match the rock block inventory (Fig. 6a).

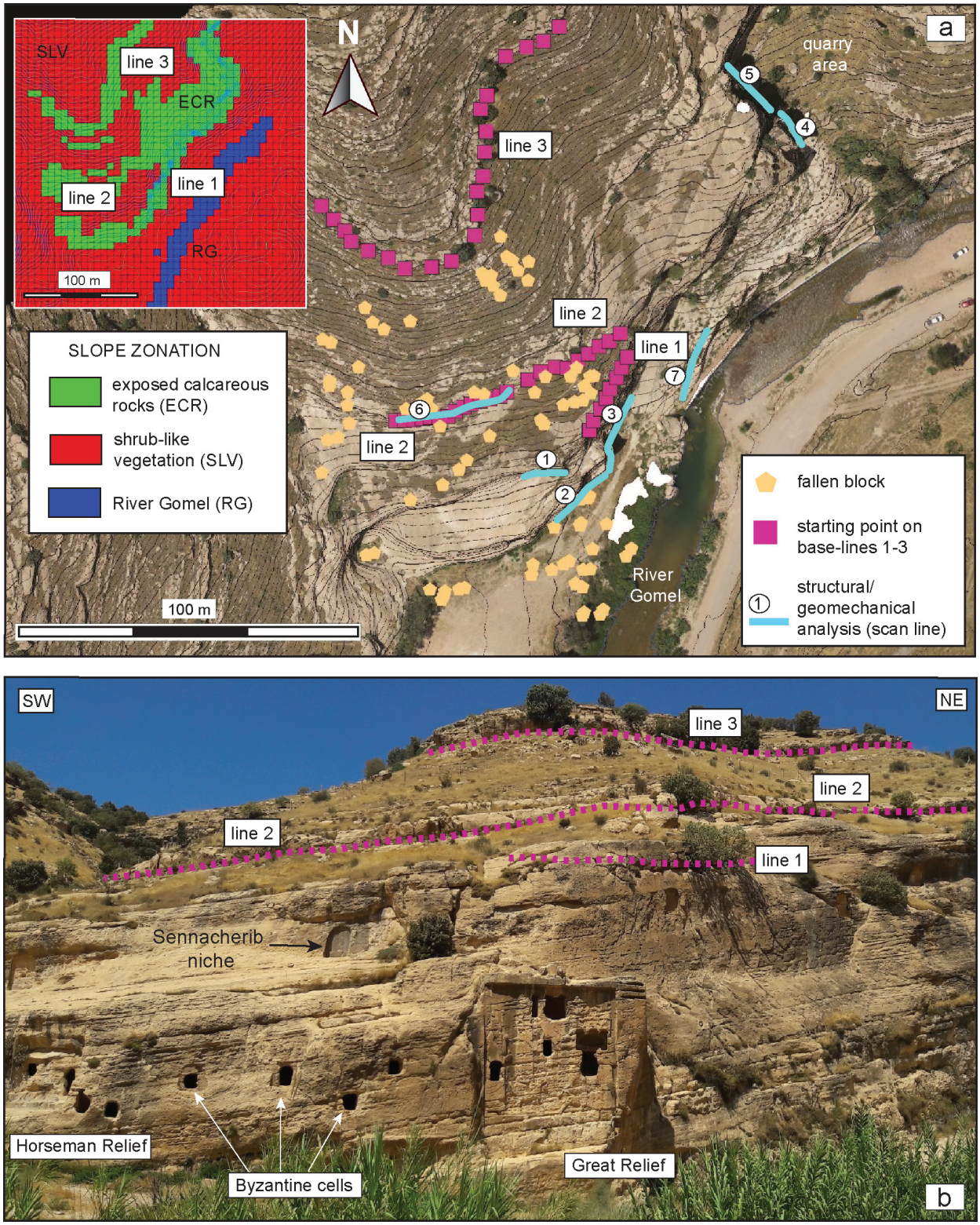


Fig. 6 - a) Base map reporting the rock block inventory and starting lines 1-3; the upper left insight shows slope zonation; b) starting lines placed along the base of escarpments found at different elevations on the Khinis slope, above the Great and Horseman relieves

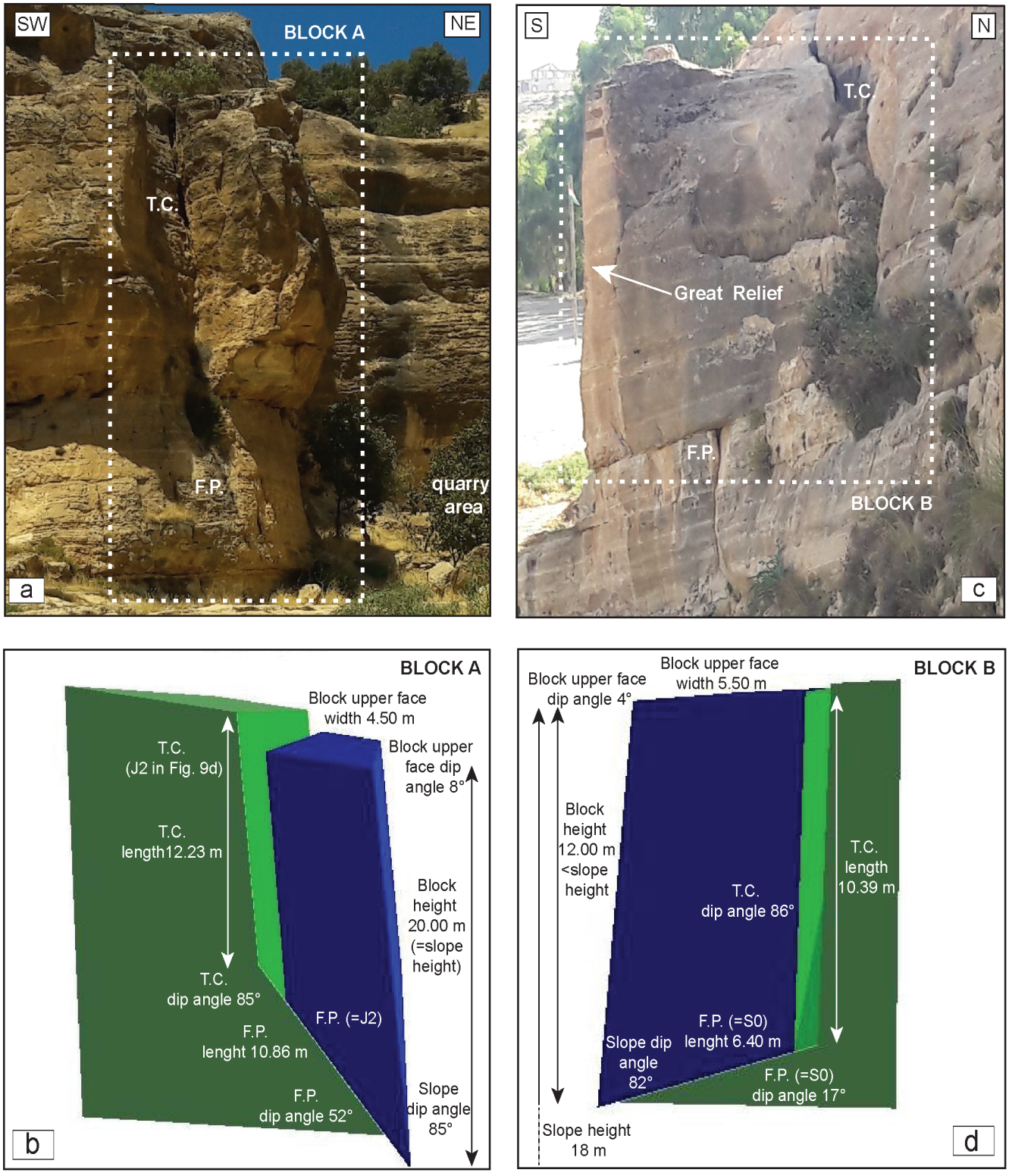


Fig. 7 - a) Rock block A on the western edge of the quarry area and b) 3D geometric reconstruction in perspective view; c) lateral view of rock block B hosting the Great Relief. and d) 3D geometric reconstruction. LEGEND: T.C.=Tension Crack; F.P.=Failure Plane

	EXPOSED CALCAREOUS ROCKS (ECR)		
	Kn	Kt	φd
Broili (1973)	0.75-0.80 (K)		
Piteau & Clayton (1987)	0.65-0.75	0.8-0.9	
Budetta & Santo (1994)	0.20	0.53	
Azzoni & De Freitas (1995)	0.51-0.92 (K)		
Azzoni *et alii* (1995)	0.75-0.90 (K)		0.40-0.45
Chau *et alii* (2002)	0.40-0.60	0.65-0.90	
Guzzetti *et alii* (2003)	0.65	0.80	0.30
Guzzetti *et alii* (2004)	0.65	0.75	0.25
Ferrari *et alii* (2013)	0.60	0.80	0.20
average min/max	0.573-0.674	0.744-0.811	0.287-0.300
average before calibration	0.623	0.777	0.293
after calibration	*0.50*	*0.60*	*0.35*
difference	*-19.24%*	*-22.68%*	*+16.28%*
	SHRUB-LIKE VEGETATION (SLV)		
	Kn	*Kt*	*φd*
Pfeiffer & Bowen (1989)	0.30-0.33	0.83-0.87	
Pfeiffer & Higgins (1990)		0.82-0.85	
Agliardi & Crosta (2003)	0.33	0.75	0.50
average min/max	0.315-0.330	0.800-0.823	0.50
average before calibration	0.315	0.812	0.50
after calibration	*0.3*	*0.5*	*0.6*
difference	*-14.28%*	*-38.42%*	*+16.67%*

Tab. 2 - Values of Kn, Kt and Φd parameters assigned to the terrain classes identified on the Khinis slope. Both averaged values for initial modelling and final values after model calibration are given, with the percentage difference

RESULTS

Geometric models of rock blocks A and B were derived from DEM analysis, reconstruction of topographic sections and field measurements; the main characteristics are summarized in Figure 7. Located at the south-west margin of the disused quarry, block A has a prismatic shape and is bounded to the rear by the combination of a sub-vertical, opened tension crack and a less steep failure plane (Fig. 7a). These joined discontinuities cut off the entire rock outcrop from the top to the bottom of the slope. Considering the length and geometric attitudes of the delimiting surfaces as well as the block shape and size (Fig. 7b), an estimated volume of approximately 900 m^3 is determined. Similarly, as a function of joint geometry, block B hosting the Great Relief on its front side (Fig. 7c) presents a length and upper face width comparable to those of block A, but a lower height being delimited downwards by a bedding surface (Fig. 7d). Therefore, its volume is slightly smaller (759 m^3) than that of block A.

Calculations of strength parameters were focused on potential failure surfaces (Tab. 1). With regard to block A, both Schmidt hammer measurements and evaluations of joint roughness were completed along the basal joint surface of the rock pillar (Figs. 7b); for block B, attention was paid to the gently dipping (17°) bedding surface S0 (Fig. 7d).

A compatibility analysis (Markland, 1972) was performed taking into account the slope geometry and characteristics of brittle deformation in the Khinis sequence (Fig. 8). The rose diagram (Fig. 8a) shows the quantitative presence of different joint systems (J1-J4). Compared to the macro-structural setting reported in Fig. 3b, there is a clear correspondence between joint systems at the slope and outcrop scales. As will be specified below, the structural analysis at site 6 will be taken into consideration for the dynamic modelling of rock fall. Structural analyses at sites 4 and 5 were taken as representative for block A (Fig. 8c). Discontinuities belonging to the J2 joint system drive planar sliding - which might also evolve to secondary toppling - as they include both the failure surface (F.S.) and tension crack (T.C.) (Fig. 8d). Joint sets J1 and J4 act as lateral limits. Wedge failures are also possible along lines of intersections between three different combinations of discontinuity surfaces (J1 and J2; J1 and J3; J2 and J4, see Fig. 8e). The joint configuration for block B was inferred from analyses at sites 2 and 3 (Fig. 8f). A sensibly reduced Φr value (17°) would be necessary to produce kinematic compatibility for sliding of the entire block along the basal bedding surface (Fig. 8f). Wedge failures within the rock mass surrounding block B are possible along intersections between joint systems J1 and J2-J4 or J2 and J3, where the slope trend changes from ENE-WSW to NNE-SSW (Fig. 8h); under this circumstance, toppling failures cannot be excluded along system J1.

After the estimation of strength parameters, reconstruction of block geometries and evaluation of kinematic compatibility for failure mechanisms, a factor of safety (*Fs*) was defined for blocks A and B adopting a limit equilibrium method under static and dry conditions (Tab. 3). The limit equilibrium is obtained when the strength of the rock block is completely engaged over the entire failure surface and the slope is at the point of collapse. This condition almost happens for the case of block A sliding over a J2 discontinuity surface (Fs=1.14) and, therefore, a situation of imminent instability is ascertained. Calculations for block B were completed both for Φr=29° (Tab. 1) and assuming a hypothetical Φr=17°, i.e the value that guarantees the kinematic compatibility

	Φr (°)	**Driving force (MN)**	**Resisting force (MN)**	**(Fs)**
Block A (P.S. along J2)	27 (estimated)	17.50	19.92	1.14
Block B (P.S. along S0)	29 (estimated)	4.71	13.16	2.79
Block B (P.S. along S0)	17 (parametric analysis)	4.11	8.18	1.99

Tab. 3 - Results of equilibrium method analyses for rock block A and B under static and dry conditions. P.S.=Planar Sliding

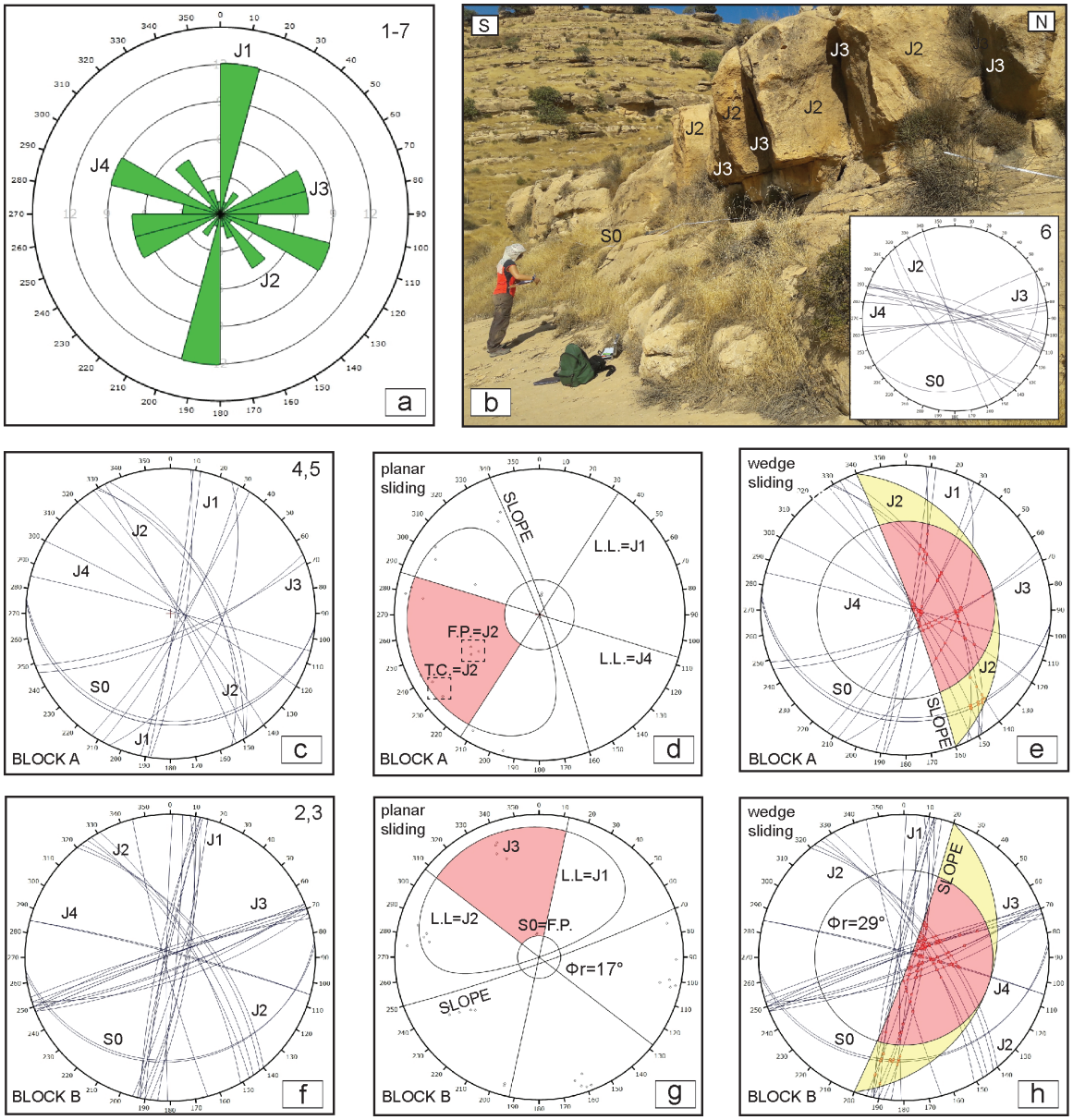


Fig. 8 - a) Rose diagram evidencing main discontinuities systems (joints and bedding) observed at the outcrop scale (sites 1-7); b) structural analysis at site 6 for design block assessment; main joint systems are reported in the lower right box; c), d), e) joint systems and kinematic analyses at sites 4-5 (block A); f), g), h) joint systems and kinematic analyses at sites 2-3 (block B)

for planar sliding along the bedding surface bounding the rock block at its base. Even with this assumption, Block B results stable (*Fs=1.99*).

Regarding the probabilistic modelling of diffuse rock falls from the Khinis slope (Figs. 5, 6), five calibration steps were completed by gradually varying the elastic restitution (*Kn*, *Kt*) and dynamic friction (*Φd*) values while holding the initial motion parameters (*V0*, *H*) constant. The rock block inventory was used as a key constraint for model validation; an ultimate simulation was considered acceptable once arrest areas predicted by the model included at least 75% of the inventoried boulders (Fig. 9a). Variations made to the elastic restitution and friction parameters were not significant, always less than 23% of the initial value, except for the *Kt* reduction (38.42%) for bedrock covered by shrub-like vegetation (Tab. 2). This fact might be explained by assuming that even the scarce vegetation in the Khinis area plays an important role in controlling rock block motion, partly retaining it during propagation.

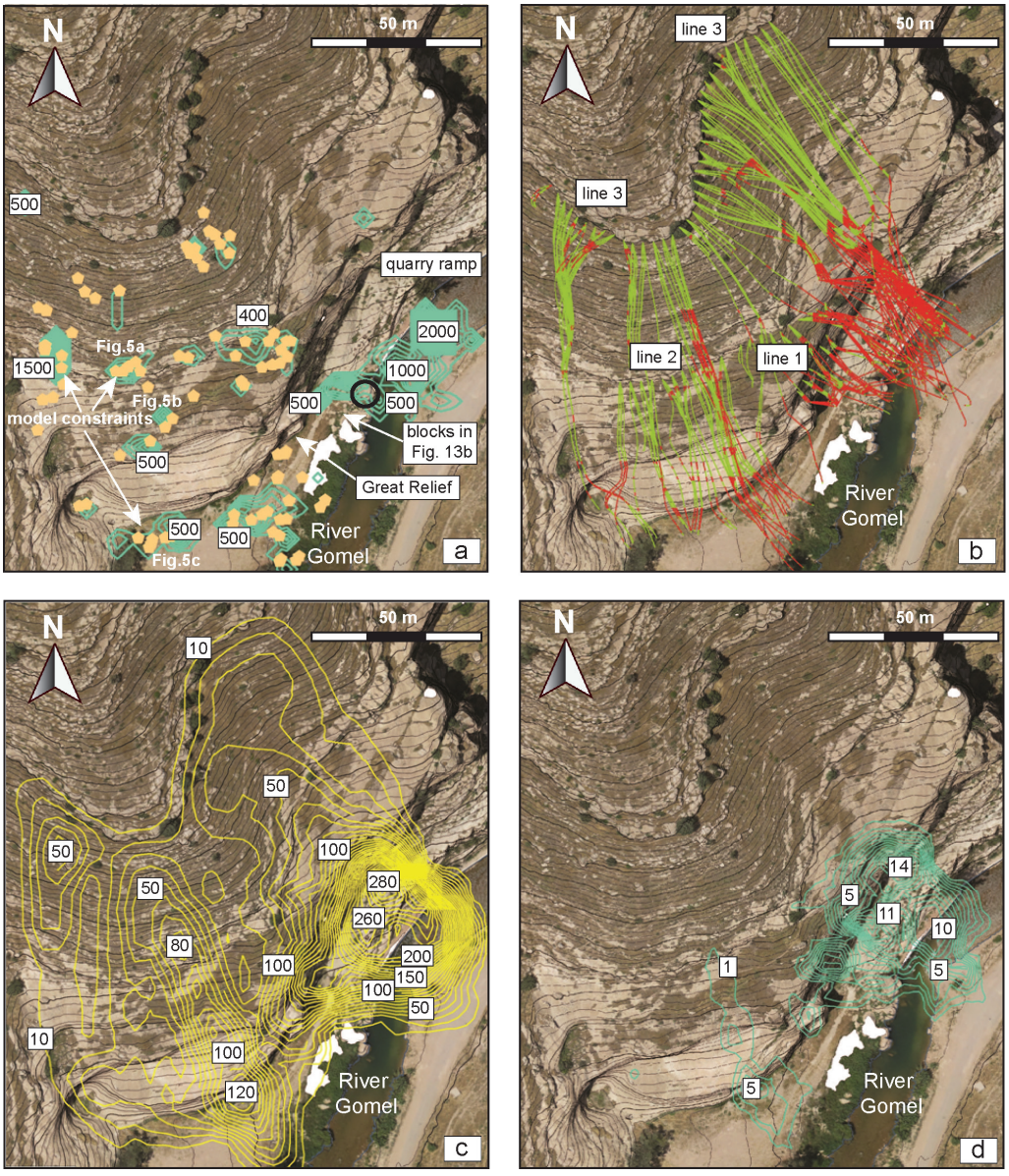


Fig. 9 - Results of the rock fall modelling: a) contour map of arrest points (ppm/m², contour interval 250·10⁶ m²) superimposed on the rock block inventory; the black circle encompasses the tilted block in Fig. 2e; b) simulated trajectories: green (pale) lines indicate rolling and sliding along slope, red (dark) lines the bouncing phase; c) contour map of the specific kinetic energy [Ecin=1/2v2 (m²/s²)], with contour interval 10 m²/s²; d) contour map of the bouncing height (h>1 m), with 1 m contour interval

Figure 9b shows the 272 simulated trajectories; in the middle and upper parts of the slope descents occur mainly by rolling or sliding. Only after passing beyond the slope break do the flight and rebound phases prevail, and rock blocks can reach the piedmont flat area and the River Gomel. Overall, the trajectories show weak angular dispersion in accordance with the regularity of the local topography.

Modelling results also outline the spatial distribution of the kinematic parameters for "dimensionless" falling boulders, namely, their speed, specific kinetic energy $Ecin=1/2v^2$ (m^2/s^2) (Fig. 9c) and rebound heights (m) (Fig. 9d).

The specific kinetic energy values do not exceed 50 m^2/s^2 on the uppermost part of the slope, whereas they increase to 100 m^2/s^2 when the boulders approach the main scarp edge and the motion changes from rolling to free-fall. This change leads to a marked increase in the kinetic energy to 280 m^2/s^2 for rock blocks potentially falling over the quarry ramp.

Finally, the distribution of rebound heights (H) of rock

block is shown in Fig. 9d, where contour lines are drawn only for values H>1 m. In agreement with the prevalence of rolling/sliding sections in the upper and middle parts of the slope (Fig. 9b), the heights of bouncing rock blocks in the western sectors are very low for long stretches and reach 5 m only during falling from the main scarp. The same features are shown for the eastern side of the slope, where the highest values (11-14 m) are again recorded only for the free-fall phase down the main scarp (red lines in Fig. 9b).

To define a plan to mitigate the geological hazards caused by the lowest magnitude rock fall processes, it was necessary to implement the kinematic model in a complete dynamic simulation, also taking into account the volumes (and therefore the masses) of the stone blocks in motion. For this purpose, a "design block" had to be established. Its shape and dimensions were determined on the basis of the geomechanical analysis conducted at site 6, along starting line 2 (see Figs. 6a, b for location). From the geometric relationships between joint systems and the bedding, a maximum reference volume of 4.5 m^3 was estimated, representing a squat columnar block 2 m high and 1.5 m wide and deep (Fig. 8b). The volume of the design block adopted disregards the process of block fragmentation that usually follows detachment from the rock scarp. Further, an overestimated size is an added safety feature.

Following the choice for the design block, protection measures were devised, which might consist of the installation of rock fall barriers. The calculations needed to establish the dimensions of such operas are reported in Table 4. The design block's mass is calculated assuming a density of 2400 kg/m^3 for the calcarenitic rocks of the Khinis sequence, which gives an estimate of 10,800 kg (10.8 tons). The block mass is then multiplied by the specific kinetic energy (m^2/s^2) indicated by simulation results in the place where the rock fall barrier will be installed, and impact energies ($kg \cdot m/s^2 \cdot m = N\ m = J$) are calculated. The mitigation plan considers the installation of eight protective barriers, each 30 m in length, to be placed where the specific Ecin values are low (Fig. 10a), with slope-parallel trends and linear overlaps (Fig. 10b). The barrier energy is expected to be higher than impact energies foreseen by the dynamic model and their heights sufficient to arrest the blocks during rebound phases (Tab. 4).

DISCUSSION

Rock falls originate from the detachment of individual blocks and evolve into subsequent down-slope movement (e.g. Evans & Hungr, 1993; Cruden & Varnes, 1996; Hungr *et alii*, 2014). Despite the limited amount of rock material involved, rock falls can cause serious damage due to their unpredictability and high velocities. In addition to communication routes, buildings and villages, elements of the cultural heritage can be threatened by and involved in these events (Tunusluoglu & Zorlu, 2009; Wang *et alii*, 2012; Di Luzio *et alii*, 2013; Fanti *et alii*, 2013; Margottini *et alii*, 2015; Dincer *et alii*, 2016; Boldini *et alii*, 2018; Di Luzio & Carfora, 2019).

In the Khinis archaeological area, rock falls of different magnitudes can occur. At the slope scale, the presence of mega-joints and very thick strata leads to the isolation within the rock mass of potentially unstable rock pillars with considerable volumes (several hundreds of m^3). The mesoscale discontinuities instead drive the diffuse detachment of smaller rock blocks from elongated escarpments, which can propagate downwards and arrive at the base of the slope.

The results of the stability analyses for blocks A and B under dry and static conditions lead to different conclusions in the two cases and to specific risk mitigation proposals for each block. Planar sliding along the bedding was investigated as a potential failure mechanism for block B. Only considering a sensible decrease in residual friction, hypothetically due to severe weathering, planar sliding becomes possible (Fig. 8g). Moreover, block detachment should be allowed by a fully developed tension crack at the rear, which is, however, discontinuous and in some sections still closed (Fig. 7c). For these two reasons, the block can be considered basically stable. On the contrary, a situation of imminent instability is summarized for block A by a very low factor of safety (*Fs*=1.14) for planar sliding along a main J2 discontinuity (Tab. 3). Among the possible factors that would trigger collapse of block A are seismic acceleration and rainfall. Figures 11a and b show the results of a sensitivity analysis for the slope-block system, which highlight the variation of instability conditions (*Fs*) following increase of interstitial water pressure or intensity of the seismic input.

	V (m^3)	Mass (kg)	Weight (N)	Max Ecin (m^2/s^2)	Impact energy (KJ)	Barrier energy (KJ)	Barrier height (m)
DB	4.5	10800	105948				
BARRIER 1				50	540	1000	3
BARRIER 2				50	540	1000	3
BARRIER 3				40	432	500	2
BARRIER 4				50	540	1000	3
BARRIER 5				30	324	500	2
BARRIER 6				40	432	500	2
BARRIER 7				30	324	500	2
BARRIER 8				40	432	500	2

Tab. 4 - Calculations of impact and absorption energies for the eight elastic barriers envisaged by the mitigation plane (assuming a 4.5 m^3 design bock DB)

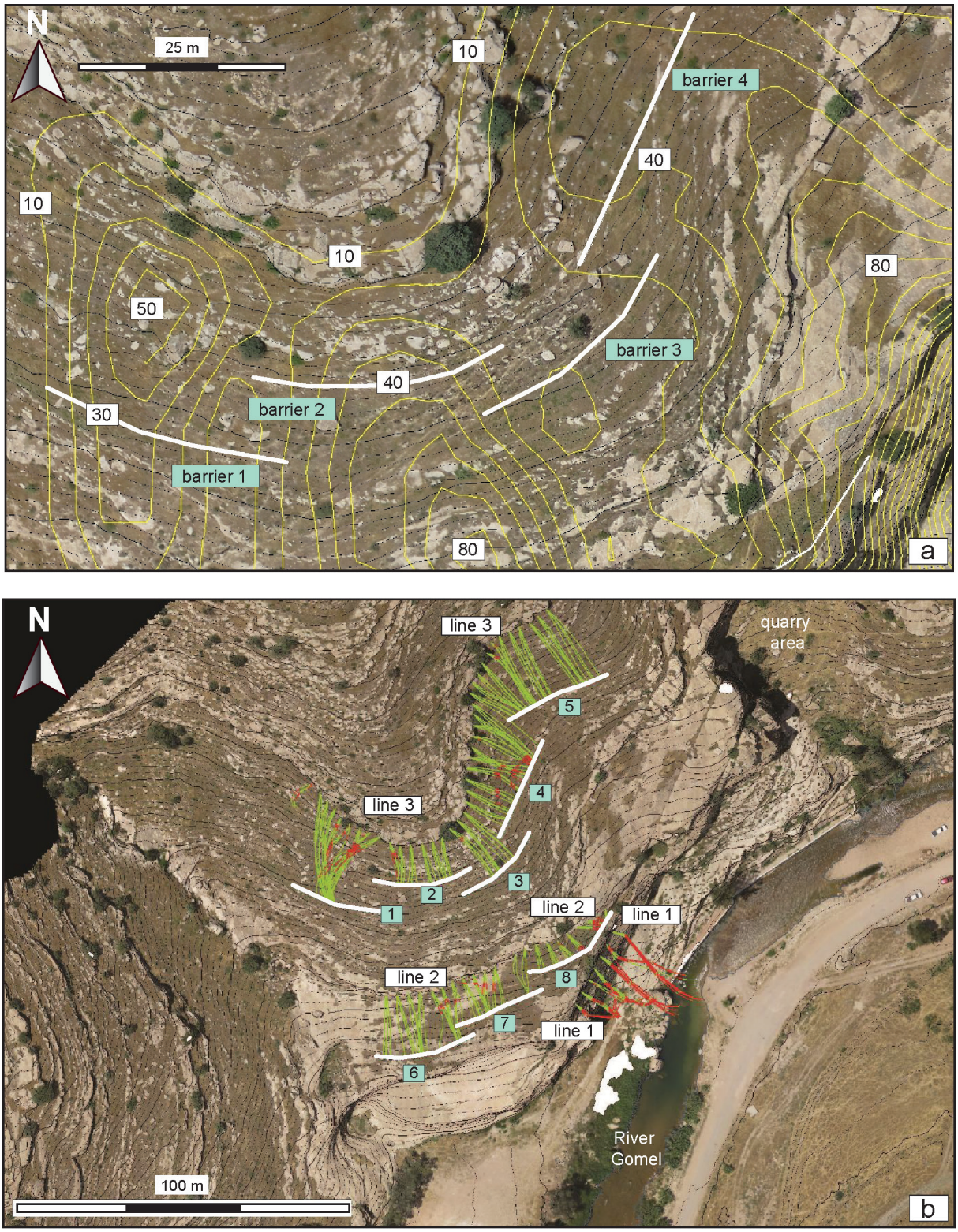


Fig. 10 - a) Installation of rock fall barriers (thick white lines) based on distribution of Ecin values; b) effects of the eight elastic barriers on rock fall propagation (except for line 1)

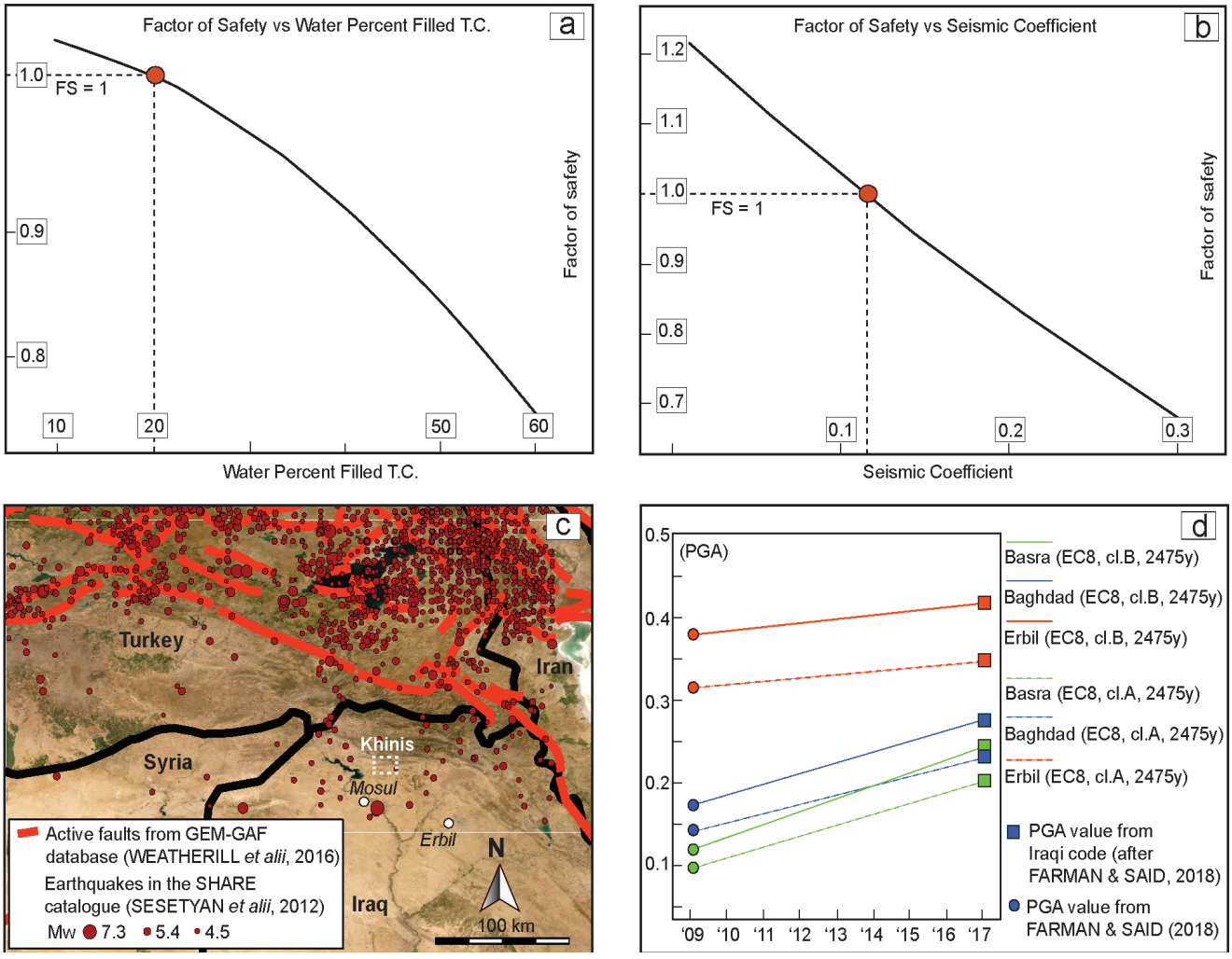


Fig. 11 - Sensitivity analysis for the slope-block A system with respect to: a) interstitial water pressure (T.C.=Tension Crack); b) seismic coefficient, expressed as a_g; c) regional seismotectonic setting. LEGEND: GEM=Global Earthquake Model; GAF=Global Active Faults database; d) PGA values expected for the Khinis site; cl.=soil class

Meteorological phenomena could lead to block failure, as water infilling only 20% of the rear tension crack (T.C. in Figs. 7a, b) would be needed (Fig. 11a). In northern Iraq, within the High Folded zone of the Zagros belt rainfall is higher than in the rest of the country, at more than 1,000 mm per year (Stefanovic, 2009; Stefanovic *et alii*, 2009). However, a recent study by Palpacelli (2019) reports pluviometric data from a measurement station placed in Erbil, 80 km east of Mosul (see upper right insight in Fig. 1a), whose position is representative of the climatic conditions of the Low Folded zone of the Zagros belt. The averaged monthly distribution of rainfall over the last twenty years ranges between 80 and 110 mm during the winter seasons, 10-60 mm over springs and autumns whereas zero rainfall are registered during dry summer times. Therefore, meteoric precipitations are not considered as the prevalent factor driving slope instability in the Khinis area.

The action of seismic shaking can be expressed by a seismic coefficient a_g, a dimensionless number that defines the seismic acceleration as a fraction of the acceleration due to gravity. The seismic force applied to the block (in a horizontal direction) may be expressed as $F=m \cdot a_g \cdot g$, where m=mass of the sliding block. In the case of block A, instability ($Fs<1$) is reached for a horizontal seismic acceleration equal to or greater than 0.12 g (Fig. 11b), which can be reached during strong earthquakes in the seismically active region of north-eastern Iraq (Sesetyan *et alii*, 2012; Weatherill *et alii*, 2016; U.S. Geological Survey, 2019), where the acknowledged maximum magnitude is between 6.0 and 7.3 (Fig. 11c). Peak ground Accelleration (PGA) reference values for the study area are available from the results of the Global Seismic Hazard Program (GSHAP) (Giardini, 1999). The GSHAP study provided 10% exceedance probability PGA's for an exposure time of 50 years (475 years return

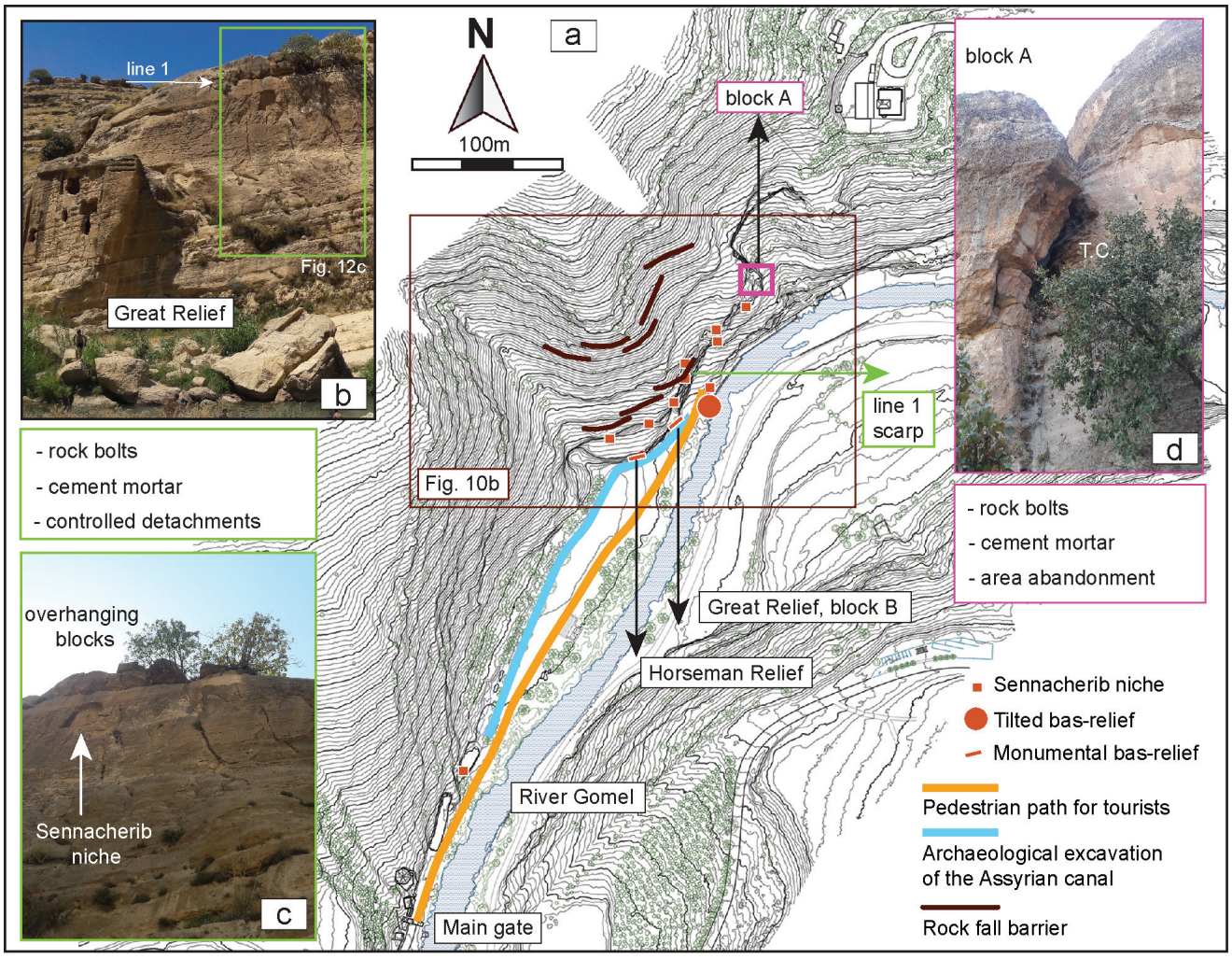


Fig. 12 - a) Planimetric map of the Khinis archaeological site with the main point of interests and intervention works for the development and protection of the area, including the installation of rock fall barriers; b), c) rock blocks along line 1 overhanging the main escarpment; d) the open tension crack (T.C.) at the rear of rock block A

period) on a worldwide scale; maximum PGA values for the Iraqi region lay in the range between 0.37 and 0.43 g. Because of the non-detailed scale of GSHAP study and the limitations in the input data, further studies were also examined. Moreover, a value of the return period (*Tr*) of 475 years for the design seismic action is generally appropriate for protection of residential buildings, while level of protection of a cultural heritage site is generally assumed higher for considerations linked to "no collapse" requirement. Thus, analyses for different return period are necessary. A recent study from Farman & Said (2018) computed PGA values for a return period of 2475 years on a B soil class in several localities and compared them to the Iraq seismic code ones, stimulating un update (Fig. 11d). These values are likely over-conservative because the area under investigation is expected to be a stiff rock-site and characterized by an A ground type according to EC8 site classification. For further comparisons, PGA values for the same return period (2475 y) but for an A ground type were computed considering the EC8 seismic coefficient S (equal to 1.2) in the formula (3): PGA (A soil class)=(PGA B soil class)/s Finally, a PGA value equal to 0.33-0.34 g (Erbil EC8 A soil class from Iraqi code) may be assumed as representative of the seismic hazard in the study area, which is greater than that required to trigger instability of rock block A (Fig. 11b).

In light of these considerations and the results of the probabilistic and dynamic modelling for low-magnitude rock falls, hazard mitigation operas are considered including different solutions with respect to the use and fruition of the archaeological site (Fig. 12). The rock fall phenomena widespread on the entire slope (Figs. 9a-d) remain the main problem, even considering the possible triggering effect of a seismic input as described above on small blocks detachments. Planned rock fall barriers must prevent

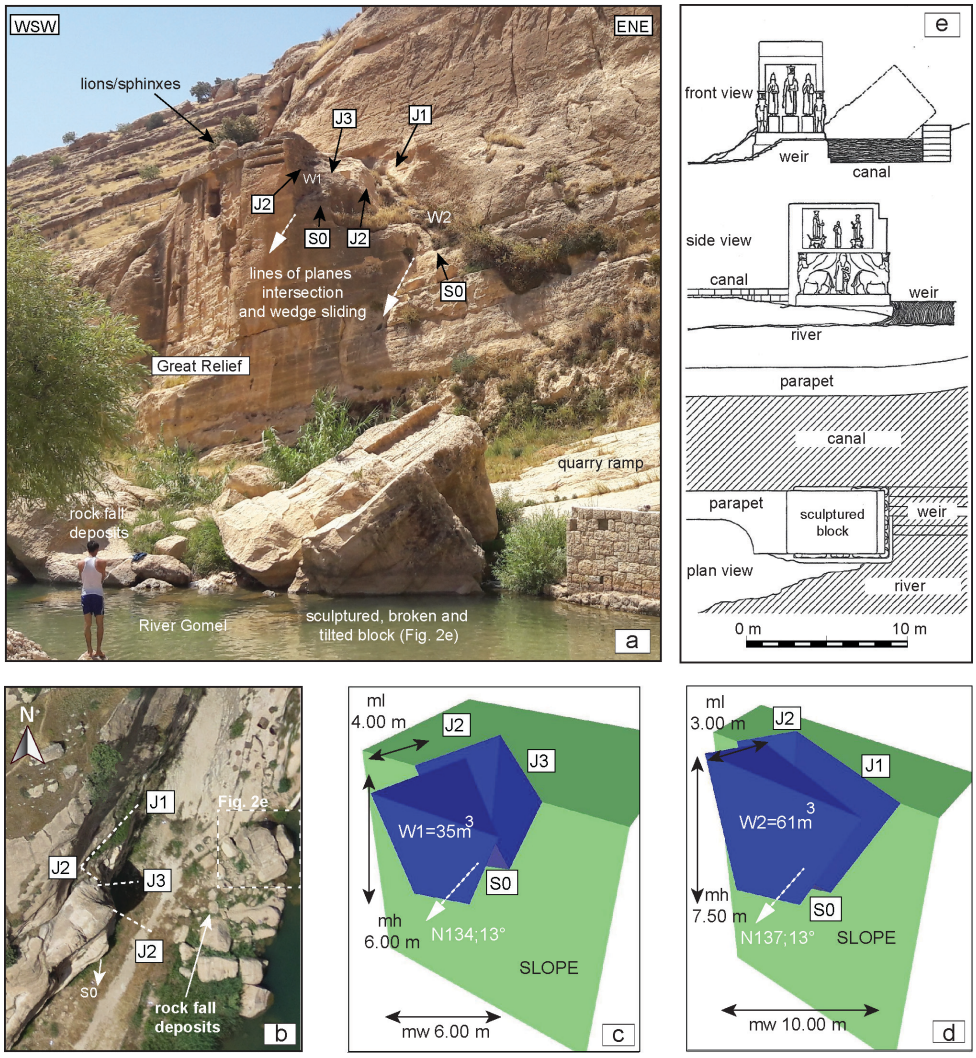


Fig. 13 - a) Rock fall deposits at the base of the Khinis slope nearby the sculptured block and wedge-shaped detachment areas W1 and W2; b) aerial image of the detachment areas and main delimiting joints; c) geometric reconstruction of wedge 1 and; d) wedge 2. LEGEND: mh=maximum height; ml=maximum length; mw=maximum width; e) tentative restoration of the canal head and the celebrative monolith by Jacobsen & Lloyd (1935)

falling blocks from invading the area of greatest interest in the archaeological site which includes the main points of interest; the barriers also should defend part of the pedestrian path and the Assyrian canal that the development project plans to bring to light again (Fig. 12a). The need to preserve the site's landscape integrity would discourage the installation of rock fall barriers to stop stone blocks that might potentially fall from the lowest of the starting lines, line 1. This line is close to the Great Relief, immediately above the upper margin of the main scarp of the Khinis slope (Figs. 6b, 12b). As a consequence, the simulated descents departing from line 1 are not deliberately opposed in modelling results (Fig. 10b). It would be advisable to adopt different solutions that might involve the installation of supports such as rock bolts in blocks showing evident conditions of instability and/or the injection of cement mortars into the bounding discontinuities. Alternatively, the controlled detachment of some overhanging rock blocks should not be excluded (Fig. 12c). At present, the development project of the archaeological site (Orazi, 2019) does not include the quarry area due to the potential instability of block B (and other small rock blocks) and the difficulty of extending the tourist path on a rough terrain. If the quarry area will not be permanently abandoned, block A could be stabilized through targeted interventions. These would include the installation of rock bolts or the injection of cement mortars within the open tension crack at the rear (Fig. 12d).

Finally, some considerations can be advanced about the possible relationships between Assyrian sculpturing and slope failures at Khinis. Structural and kinematic analyses at sites 2 and 3 outline possible wedge failures from the slope near the

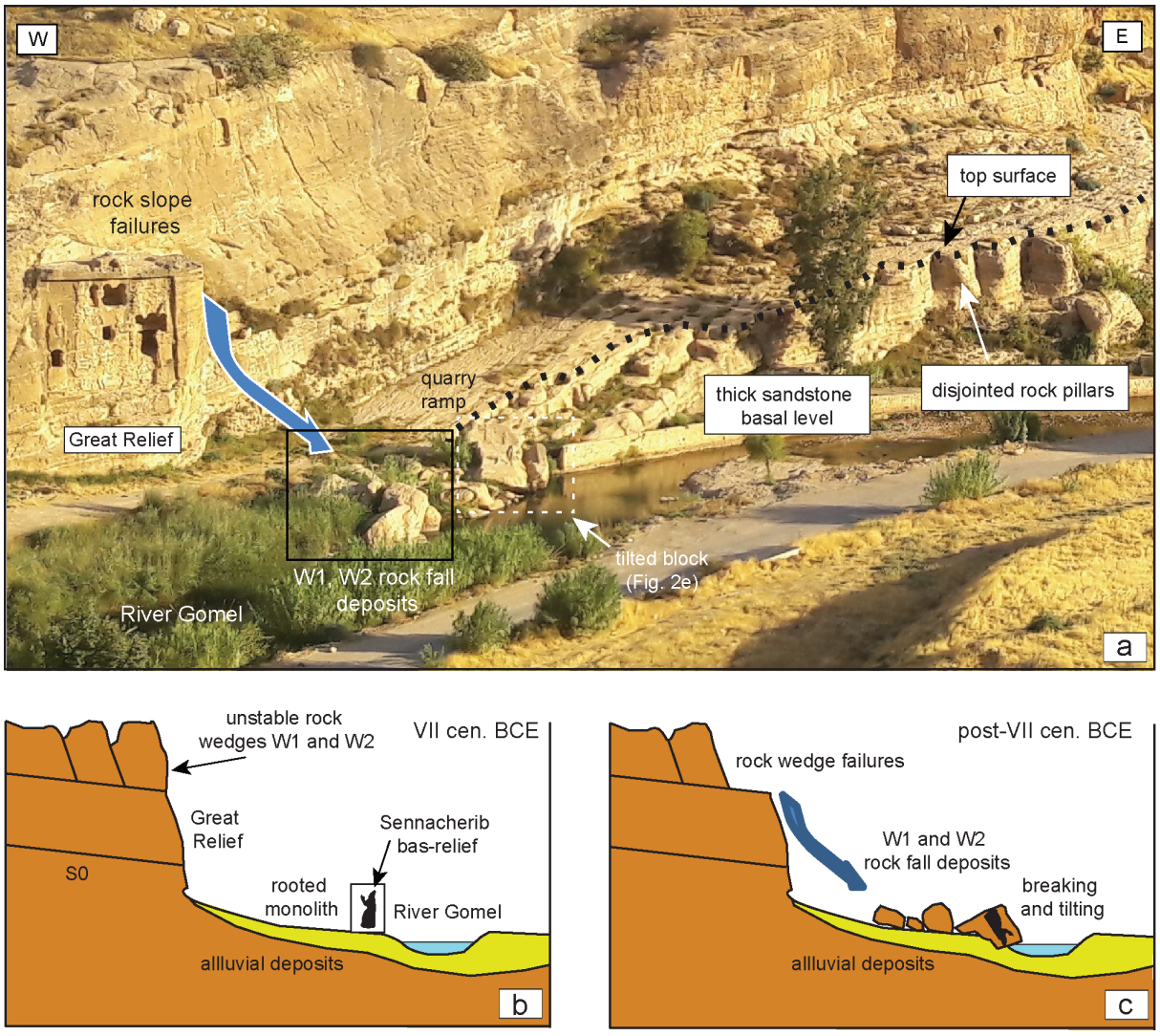


Fig. 14 - a) Panoramic view showing the tilted block, the thick basal level and rock fall deposits W1 and W2; b) Assyrian sculpturing of the Khinis slope and the rooted monolith; c) W1 and W2 rock fall events

Great Relief (Fig. 8h). Indeed, on the eastern side of block B, two wedge-shaped scars can be observed, namely W1 and W2. These scars are delimited by mega-joints belonging to the J1, J2 and J3 systems (Figs. 13a, b). The geometric reconstructions shown in Figures 13c and d allowed us to assess missing volumes of approximately 35 m^3 and 61 m^3 for wedges 1 and 2, respectively. Related rock fall deposits were found along the River Gomel, lying outside the accumulation areas outlined by the 3D modelling (Fig. 9a) and near the tilted block bearing bas-reliefs sculptured on its faces (Fig. 2e). This last block was once part of a huge sculptured monolith (Fig. 13e); its restoration indicated an overall volume of approximately 120 m^3 (Jacobsen & Lloyd, 1935).

Considering the different volume and shape, the explanation that the giant monolith was derived by sculpturing of the rock fall deposits generated from the wedge-shaped scars W1 and W2 can be excluded. It is likely that the original monolith was rooted in the geological bedrock, more precisely in the thick sandstone layer at the base of the Khinis sequence, whose top boundary corresponds to the quarry ramp surface. This layer is characterized by disjointed rock pillars of similar size (Fig. 14a).

The rooted block was sculptured during the VIII-VII centuries BCE, contemporaneously with the Great Relief (Fig. 14b). Successive rock slope failure events from the W1 and W2 source areas hypothetically caused the main damage as wedge-shaped blocks detached from the slope edge, hit and broke the monolith and eventually tilted it (Fig. 14c). Other causes for the monolith's breakage and tilting might be considered, such as earthquakes or progressive fluvial erosion of the rock base.

CONCLUSION

The Khinis archaeological site in Kurdistan (north-eastern Iraq) testifies to the great works of canalization of the river waters flowing from the Zagros belt towards the land of Nineveh, which was completed during the reign of Assyrian king Sennacherib (VIII-VII centuries BCE). The site preserves a large complex of rock sculptures created for the celebration of the canalization opera. However, the rocky slope within which Assyrian bas-reliefs were carved is subject to active rock fall processes that can compromise the development of the area and represent a serious risk for visitor safety.

Stability analyses of very large rock pillars isolated by mega-joints outlined an impending collapse from the rock edge of a disused quarry. The event would involve the sliding of a 900 m^3 rock mass and might be triggered by earthquakes or, secondarily, rainfall events. The same analysis, based on the limit-equilibrium method, indicated a condition of stability for the 760 m^3 rock panel bearing on its outer edge the Great Relief, an outstanding bas-relief imaging King Sennacherib and the Assyrian gods. Close to the Great Relief, slope analysis identified a pair of wedge-shaped scars with missing rock volumes ranging between 35 and 60 m^3. These scars were recognized as the detachment areas of rock fall deposits that likely determined the breakage and tilting of a former sculptured monolith into the River Gomel. The monolith was originally rooted in the geological bedrock within a thick basal sandstone layer.

Rock fall processes in the Khinis area also involved moderate-sized blocks (few cubic metres) that can detach from rocky escarpments extending from the middle and upper parts of the slope. The results of a 3D probabilistic model revealed block trajectories, arrest zones and spatial distributions of kinematic parameters along the slope. Following the definition of a design block, a remediation plan was defined, including the installation of elastic barriers. The aim of reducing the geological hazards includes different solutions. These are part of a development project for the entire archaeological area which will be proposed for inclusion on the UNESCO World Heritage List as one of the most important elements of Sennacherib's irrigation system.

ACKNOWLEDGEMENTS

The authors are grateful to Prof. Daniele Morandi Bonacossi (Udine University), Head of the Italian Archaeological Mission leading the project "Land of Nineveh - Training for the enhancement of the cultural heritage of Northern Kurdistan" entrusted by MAECI, the Italian Ministry of Foreign Affairs and International Cooperation. The territorial and architectural documentation has been conducted under the supervision of Arch. Roberto Orazi (CNR-ITABC) who also is the Director of the project for the "Archaeological Park of Sennacherib Irrigation Network".

Financial support was provided by MAECI (Prof. Morandi Bonacossi) and secondarily by MIBAC, the Italian Ministry for Cultural Heritage and Activities (Arch. Orazi). The research was also supported by the Ministry of Education, Universities and Research (MIUR) as part of the project "Archaeological Landscapes of Mesopotamia between Prehistory and the Islamic Period: Formation, Transformation, Protection and Enhancement".

REFERENCES

Agliardi F. & Crosta G.B. (2003) - *High resolution three-dimensional numerical modeling of rockfalls*. Int. J. Rock Mech. Mining Sci., **40**: 455-471. https://doi.org/10.1016/S1365-1609(03)00021-2.

Alavi M. (2004) - *Regional stratigraphy of the Zagros Fold-Thrust Belt of Iran and its proforeland evolution.* American Journal of Science, **304**: 1-20. https://doi.org/10.2475/ajs.304.1.1

Alavi M. (2007) - *Structures of the Zagros fold-thrust belt in Iran.* American Journal of Science, **307**: 1064-1095. https://doi.org/10.2475/09.2007.02.

Al-Mashaikie S.Z.A.K. & Latif R.M.A. (2017) - *Sedimentology and Lithostratigraphy of the Pila Spi Formation in Koi Sanjaq area, NE Iraq; new insight for depositional environment and basin configuration.* Iraqi Journal of Science, **58** (2A): 666-686. https://doi.org/10.24996.ijs.2017.58.2A.10.

Aqrawi A.M., Goff J.C., Horbury A.D. & Sadooni F.N. (2010, Eds.) - *The Petroleum Geology of Iraq*. Scientific Press, Beaconsfield, United Kingdom.

Azzoni A. & De Freitas M.H. (1995) - *Experimentally gained parameters, decisive for rock fall analysis.* Rock Mechanics and Rock Engineering, **28**: 111-124. https://doi.org/10.1007/BF01020064.

Azzoni A., La Barbera G. & Zaninetti A. (1995) - *Analysis and prediction of rockfalls using a mathematical model*. Int. J. Rock Mech. Mining Sci., **32**: 709-724. https://doi.org/10.1016/0148-9062(95)00018-C.

Bachmann W (1927, Eds.) - *Felsreliefs in Assyrien, Bawian, Maltai und Gundük*. Hinrichs, Leipzig (Germany)

Bagg A.M. (2000) - *Irrigation in Northern Mesopotamia: water for the Assyrian capitals (12th-7th centuries BC)*. Irrigation and Drainage Systems, **14**: 301-324. https://doi.org/10.1023/A:1006421000423.

BÄR J. (2006) - *New Observations on Khinnis/Bavian (Northern Iraq).* State Archives of Assyria Bulletin, **15**: 43-92.

Barton N. & Choubey V. (1977) - *The shear strength of rock joints in theory and practice*. Rock Mechanics, **10**: 1-54. https://doi.org/10.1007/BF01261801.

Blanc E.J.P., Allen M.B., Inger S. & Hassani H. (2003) - *Structural styles in the Zagros Simple Folded Zone, Iran*. Journal of the Geological Society, **160** (3): 401-412. http://dx.doi.org/10.1144/0016-764902-110.

Boldini D., Guido G.L., Margottini C. & Spizzichino S. (2018) - *Stability analysis of a large-volume block in the historical rock-cut city of Vardzia*

(Georgia). Rock Mechanics and Rock Engineering, **51**: 341-349. https://doi.org/10.1007/s00603-017-1299-7.

Broili L. (1973) - *In situ tests for the study of rockfall*. Geologia applicata e idrogeologia, **8** (1): 105-111.

Bruce I.G., Cruden D.M. & Eaton T.M. (1989) - *Use of a tilting table to determine the basic friction angle of hard rock samples.* Canadian Geotechnical Journal, **26** (3): 474-479. https://doi.org/10.1139/t89-060.

Buday T. & Jassim S.Z. (Eds.) (1987) - *The Regional Geology of Iraq: tectonism, magmatism, and metamorphism.* GEOSURV Publication, Baghdad, Iraq.

Budetta P. & Santo A. (1994) - *Morphostructural evolution and related kinematics of rockfalls in Campania (southern Italy): a case study.* Engineering Geology, **36**: 197-210. https://doi.org/10.1016/0013-7952(94)90004-3.

Chau K.T., Wong R.H.C. & Wu J.J. (2002) - *Coefficient of restitution and rotational motions of rockfall impacts.* Int. J. Rock Mech. Mining Sci, **39**: 69-77. https://doi.org/ 10.1016/S1365-1609(02)00016-3.

Crosta G.B. & Agliardi F. (2004) - *Parametric evaluation of 3D dispersion of rockfall trajectories.* Nat. Hazards Earth Syst. Sci., **4**: 583-598. https://doi.org/10.5194/nhess-4-583-2004.

Cruden D.M. & Hu X.Q. (1988) - *Basic friction angles of carbonate rocks from Kananaskis country.* Canadian Bull. Int. Assoc. Eng. Geol., **38**: 55-59.

Cruden D.M. & Varnes D.J. (1996, EDS.) - *Landslide types and processes.* Transportation Research Board, Special Report 247, National Academy Press, Washington, D.C.

Csontos L., Sasvári Á., Pocsai T., Kósa L., Salae. A.T. & Ali A. (2012) - *Structural evolution of the north-western Zagros, Kurdistan Region, Iraq: implications on oil migration*. GeoArabia, **17** (2): 81-116.

Di Luzio E., Bianchi Fasani G. & Bretschneider A. (2013) - *Potential rockfalls and analysis of slope dynamics in the Palatine archaeological area.* Geologica Acta, **11** (2): 245-264. https://doi.org/10.1344/105.000001834.

Di Luzio E. & Carfora P. (2019 - Eds.) - *Approcci multidisciplinari per la ricostruzione del paesaggio di una grande strada romana. La via Appia al valico degli Aurunci.* Claudio Grenzi Editore, Foggia, Italy.

Dinçer I., Orhan A., Frattini P. & Crosta G.B. (2016) - *Rockfall at the heritage site of the Tatlarin Underground City (Cappadocia, Turkey)*. Natural Hazards, **82**: 1075-1098. https://doi.org/10.1007/s11069-016-2234-z.

Dorren L. (2003) - *A review of rockfall mechanics and modelling approaches*. Progress in Physical Geography, **27** (1): 69-87. https://doi.org/10.1191/0309133303pp359ra.

Evans S.G. & Hungr O. (1993) - *The assessment of rockfall hazard at the base of talus slopes.* Canadian Geotechnical Journal, **30**: 620-636. https://doi.org/10.1139/t93-054.

Fales F. & Del Fabbro R. (2014) - *Back to Sennacherib's aqueduct at Jerwan: a reassessment of the textual evidence.* Iraq, **76**: 65-98. https://doi.org/10.1017/irq.2014.8.

Fanti R., Gigli G., Lombardi L., Tapete D. & Canuti P. (2013) - *Terrestrial laser scanning for rockfall stability analysis in the cultural heritage site of Pitigliano (Italy)*. Landslides, **10** (4): 409-420 https://doi.org/10.1007/s10346-012-0329-5.

Farman S.M.S. & Said A.I. (2018) - *Updated probabilistic seismic hazard assessment for Iraq/2018.* Civil Engineering Journal, **4** (7): 1610-1628. https://doi.org/:10.28991/cej-0309199.

Ferrari F., Giani G.P. & Apuani T. (2013) - *Towards the comprehension of rockfall motion, with the aid of in situ tests.* Italian Journal of Engineering Geology and Environment, Book series **6**: 163-171. https://doi.org/10.4408/IJEGE.2013-06.B-13.

Ghasemi A. & Talbot C.J. (2005) - *A new tectonic scenario for the Sanandaj-Sirjan Zone (Iran).* Journal of Asian Earth Sciences, **26**: 683-693. https://doi.org/10.1016/j.jseaes.2005.01.003.

Giardini D. (1999) - *The Global Seismic Hazard Assessment Program (GSHAP)-1992/1999*. Annali di Geofisica, **42** (6). https://doi.org/10.4401/ag-3780.

Gonzalez De Vallejo L.I., Ferrer M., Ortuno L. & Oteo C. (Eds.) (2005) - *Geoingegneria*. Pearson Education, Turin, Italy

Goodman R.E. (Ed.) (1989) - *Introduction to rock mechanics.* 2nd ed. Wiley J. & Sons, New York, USA.

Guzzetti F., Crosta G., Detti R. & Agliardi F. (2002) - *STONE: a computer program for the three-dimensional simulation of rock-falls.* Computers and Geosciences, **28** (9):1079-1093. https://doi.org/10.1016/S0098-3004(02)00025-0.

Guzzetti F., Reichenbach P. & Wieczorek G.F. (2003) - *Rockfall hazard and risk assessment in the Yosemite Valley, California, Usa.* Natural Hazards and Earth System Sciences, **3**: 491-503. https://doi.org/10.5194/nhess-3-491-2003.

Guzzetti F., Reichenbach P. & Ghigi S. (2004) - *Rockfall hazard and risk assessment along a transportation corridor in the Nera Valley, Central Italy.* Environmental Management, **34**: 191-208. https://doi.org/10.1007/s00267-003-0021-6.

Hoek E. & Bray J.W. (1981) - *Rock slope engineering.* 3rd ed. The Institution of Mining and Metallurgy, London, United Kingdom.

Hungr O., Leroueil S. & Picarelli L. (2014) - *The Varnes classification of landslide types, an update.* Landslides, **11** (2): 167-194. https://doi.org/10.1007/s10346-013-0436-y.

Koshnaw R.I., Horton B.K., Stockli D.F. & Kendall J.J. (2017) - *Neogene shortening and exhumation of the Zagros fold-thrust belt and foreland basin in the Kurdistan region of northern Iraq*. Tectonophysics, **694**: 332-355. https://doi.org/doi:10.1016/j.tecto.2016.11.016

Jacobsen T. & Lloyd S. (Eds.) (1935) - *Sennacherib's Aqueduct at Jerwan.* The University of Chicago Press, Chicago, USA.

Jassim S.Z. & Goff J.C. (2006) - *Geology of Iraq.* 1st ed. Dolin, Prague and Moravian Museum, Brno, Czech Republic.

Lan H., Martin C.D. & Lim CH (2007) - *Rock fall analyst: a GIS extension for three-dimensional and spatially distributed rock fall hazard modelling*. Computer Geosciences, **33**: 262-279 https://doi.org/10.1016/j.cageo.2006.05.013.

Lin L. & Lan H (2015) - *Probabilistic modeling of rockfall trajectories: a review.* Bulletin of Engineering Geology and the Environment, **74** (4): 1163-1176. https://doi.org/10.1007/s10064-015-0718-9

Le Garzic E., Vergés J., Sapin F., Saura E., Meresse F. & Ringenbach J.C. (2019) - *Evolution of the NW Zagros Fold-and-Thrust Belt in Kurdistan Region of Iraq from balanced and restored crustal-scale sections and forward modeling.* Journal of Structural Geology, **124**: 51-69. https://doi.org/10.1016/j.jsg.2019.04.006.

Malinverni E.S., Pierdicca R., Bozzi C.A., Colosi F. & Orazi R. (2017) - *Analysis and Processing of Nadir and Stereo VHR Pleiadés Images for 3D Mapping and Planning the Land of Nineveh, Iraqi Kurdistan.* In: Tapete D. (Ed.). Remote Sensing and Geosciences for Archaeology. Geosciences, **7** (80), 1-18. https://doi:10.3390/geosciences7030080.

Margottini C., Antidze N., Corominas J., Crosta G.B., Frattini P., Gigli G., Giordan D., Iwasaky I., Lollino G., Manconi A., Marinos P., Scavia C., Sonnessa A., Spizzichino D. & Vacheishvili N. (2015) - *Landslide hazard, monitoring and conservation strategy for the safeguard of Vardzia Byzantine monastery complex, Georgia.* Landslides, **12**: 193-204. https://doi.org/10.1007/s10346-014-0548-z.

Morandi Bonacossi D. (2018) - *Water for Nineveh. The Nineveh irrigation system in the regional context of the 'Assyrian Triangle': a first geoarchaeological assessment.* In: Kühne H. (Ed.) (2018) Water for Assyria. Studia Chaburensia series 7: 77-115. Verlag Publisher, Harrassowitz, Wiesbaden, Germany.

Oates D. (Ed.) (1968) - *Studies in the ancient history of Northern Iraq.* Oxford University Press, London.

Orazi R. (Ed.) (2019) - *The archaeological environmental park of Sennacherib's irrigation network*. Forum Editrice, Udine, Italy.

Othman A.A. & Gloaguen R. (2013) - *Automatic extraction and size distribution of landslides in Kurdistan region, NE Iraq*. Remote Sensing, **5**: 2389-2410. https://doi.org/10.3390/rs5052389.

Palpacelli S. (2019) - *Hydraulic and hydrogeological studies of the Khinis and Maltai archaeological areas.* In: Orazi R. (Ed.) (2019). *The archaeological environmental park of Sennacherib's irrigation network*. 181-193, Forum Editrice, Udine, Italy.

Panizza M. (2001) - *Geomorphosites: concepts, methods and examples of geomorphological survey.* Chinese Science Bulletin, **46**: 4-6.

Panizza M. & Piacente S. (2005) - *Geomorphosites: a bridge between scientific research, cultural integration and artistic suggestion.* Italian Journal of Quaternary Sciences, **18** (1): 3-10.

Pfeiffer T.J. & Bowen T.D. (1989) - *Computer simulation of rockfalls.* Bulletin of the Association of Engineering Geologists, **26**: 135-146. https://doi.org/10.2113/gseegeosci.xxvi.1.135.

Pfeiffer T.J. & Higgins J.D. (1990) - *Rockfall hazard analysis using the Colorado rockfall simulation program.* Transportation Research Record 1288: pp 117-126.

Piteau D.R. & Clayton R. (1987) - *Computer rockfall model.* Proc. ISMES Meeting on Rockfall Dynamics and Protective Works Effectiveness, 123-125, Bergamo, Italy.

Polla A.K. (2011) - *Interpretation of new facies in the Pila Spi formation (Middle-Late Eocene) in Sulaimaniyah, NE Iraq.* Iraqi Bulletin of Geology and Mining, **7** (3): 33-45.

Reade J.E. (1978) - *Studies in Assyrian Geography. Part 1: Sennacherib and the Waters of Nineveh; Part 2: notes on the inner provinces*. Revue d'Assyriologie, **72** (47-72): 157-180.

Reade J.E. & Anderson J.R. (2013) - *Gunduk, Khanes, Gaugamela, Gali Zardak: notes on Navkur and nearby rock-cut sculptures in Kurdistan*. Zeitschrift für Assyriologie, **103** (1): 68-122.

Reynard E. (2005) - *Geomorphosites et paysages.* Geomorphologie: relief, processus, environnement, **11** (3): 181-188.

Reynard E. & Giusti C. (2018) - *The landscape and the cultural value of geoheritage*. In: Reynard E. & Brilha J. (Eds.) (2018). Geoheritage: assessment, protection and management, 147-166, Elsevier, Amsterdam, The Netherlands.

Ritchie A.M. (1963) - E*valuation of rockfall and its control.* Highway Research Board Record 17: 13-28.

Rocscience Software suite (Dips, Plane, Topple, Wedge) - License code: 8324A.

Rotomap software suite - Geo&Soft International - License code: T3N2781.

Scioldo G. (2006) - *User guide: ISOMAP and ROTOMAP - 3D surface modelling and rockfall analysis.* http://www.geoandsoft.com/english/download.htm.

Sesetyan K., Demircioglu M., Rovida A., Albini P., Stucchi M., Zare M., Viganò D. & Locati M. (2012) - *SHARE-CET, the SHARE earthquake catalogue for Central and Eastern Turkey complementing the SHARE European Earthquake Catalogue (SHEEC).* SHARE | Work Package 3 | Task 3.1 Seismic Hazard Harmonization in Europe Seventh Framework Programme (FP7). https://www.emidius.eu/SHEEC/2.

Sissakian V.K.& Fouad S.F. (2012) - *Geological Map of Iraq.* 4th ed. GEOSURV Publication, Baghdad, Iraq

Stevanovic Z. (2009) - *Groundwater management in northern Iraq.* Hydrogeology Journal, **17** (2): 367-378. https://doi.org/10.1007/s10040-008-0331-0

Stevanovic Z., Iurkiewicz A. & Maran A. (2009) - *New insights into karst and caves of north-western Zagros (Northern Iraq).* Acta Carsologica, **38** (1):

83-96. https://doi.org/10.3986/ac.v38i1.138.

Tunusluoglu M.C. & Zorlu K. (2009) - *Rockfall hazard assessment in a cultural and natural heritage (Ortahisar Castle, Cappadocia, Turkey)*. Environmental Geology, **56** (5): 963-972. https://doi.org/10.1007/s00254-008-1198-z.

Ulusay J.A. & Hudson J.A. (2007) - *The complete ISRM suggested methods for rock characterization, testing and monitoring*. 1974-2006. International Society for Rock Mechanics, Ankara, Turkey.

Ur J. (2005) - *Sennacherib's northern Assyrian canals: new insights from satellite imagery and aerial photography*. Iraq, **67** (1): 317-345. https://doi.org/10.1017/S0021088900001418.

U.S. Geological Survey (2019) - *Earthquake catalog.* Eartquake Hazard Program (https://earthquake.usgs.gov/earthquakes/search/).

Yousif L.D. & Shakir A.M. (2015) - *Assessment of rockfall hazards on Mirawa-Mawaran main road, Kurdistan region, N Iraq. Iraqi* Bulletin of Geology and Mining, **11** (3): 107-116.

Waltham A.C. (Ed.) (2009) - *Foundations of Engineering Geology.* 3rd ed. Spon Press, Taylor and Francis, London, United Kingdom.

Wang X., Zhang L., Wang S., Agliardi F., Frattini P., Crosta G.B. & Yang Z. (2012) - *Field investigation and rockfall hazard zonation at the Shijing Mountains Sutra caves cultural heritage (China).* Environmental Earth Science, **66**: 1897-1908. https://doi.org/10.1007/s12665-011-1414-0.

Weatherill G.A., Pagani M. & Garcia J. (2016) - *Exploring earthquake databases for the creation of magnitude-homogeneous catalogues: tools for application on a regional and global scale.* Geophysical Journal International, **206** (3), 1652-1676. https://doi.org/10.1093/gji/ggw232.

Zebari M. (2013) - *Geometry and evolution of fold structures within the High Folded Zone: Zagros Fold-Thrust Belt, Kurdistan Region-Iraq*. Dissertation, University of Nebraska-Lincoln. USA.

Received September 2019 - Accepted December 2019